THE ASTRONOMICAL JOURNAL VOLUME 96, NUMBER 2 AUGUST 1988

# SUBARCSECOND-RESOLUTION RADIO OBSERVATIONS OF SIXTEEN CORE-DOMINATED QUASARS AND ACTIVE GALACTIC NUCLEI

CHRISTOPHER P. O'DEA<sup>a)</sup> AND RICHARD BARVAINIS<sup>b)</sup>
National Radio Astronomy Observatory, c) Edgemont Road, Charlottesville, Virginia 22903

## PETER M. CHALLIS<sup>d)</sup>

Astronomy Department, University of Michigan, c) Ann Arbor, Michigan 48109

\*\*Received 20 January 1988; revised 14 April 1988

#### **ABSTRACT**

We present subarcsecond-resolution VLA observations at wavelengths of 6, 2, and 1.3 cm of 16 coredominated quasars and active galactic nuclei. We have detected a wide variety of structures, including one-sided jets, short extensions to the cores, which may indicate the presence of jets, and secondary components, which may be hotspots and/or the brighter parts of lobes. The magnetic fields in the jets are always initially parallel to the jet axis at the base of the jets and continue to be parallel for most sources, even as the jets bend. This magnetic field structure is consistent with an explanation for the wiggles of the jets in 1823 + 568 and 2037 + 511 in terms of helical instabilities in a fluid beam. However, we cannot rule out precession of the central engine with subsequent ballistic motion of the ejecta as the cause of the apparent wiggles. We find no tendency for the 1.3 cm polarization position angle of the core to be perpendicular to the milliarcsecond radio-source axis. This is in contrast with previous results based on lower-frequency observations. The discrepancy may be caused by increased variability or by a lack of extended polarized structure whose B field is aligned with the VLBI jet at short wavelengths. The powers of the extended emission of these objects are sufficiently large that they should exhibit one-sided jets containing magnetic fields predominantly aligned with the axis of the jet. Our observations are basically consistent with these properties. Based on the large powers, these sources should also have classical double morphology. However, consistent with previous work, we find that the extended structure of these core-dominated sources is more asymmetric than the extended structure of lobe-dominated sources. The asymmetry between opposing sides of the sources suggests that, if the jets are intrinsically symmetric, they have bulk velocities  $\beta \gtrsim 0.2-0.7$ . We note that previous limits on the expected Doppler boosting in the extended structure based on advance speeds of the hotspots may be in error. We point out that numerical hydrodynamic models of hotspots as well as analytic arguments suggest that the flow speeds through the hotspots and lobes may be a substantial fraction of the initial jet velocity. Thus, Doppler boosting of the extended structure may be important and should be considered in unifying schemes for radio sources.

# I. INTRODUCTION

The relationship between lobe-dominated and core-dominated quasars is unclear. One possibility is that the two types of sources represent opposite ends of the distribution of intrinsic properties. Another, much discussed possibility is that the two types of sources are intrinsically similar (i.e., that they come from the same parent population). In this second hypothesis, the cores, and possibly to a lesser extent the larger-scale structures, have relativistic bulk velocities which cause the apparent flux density to increase as the observer's inclination to the radio-source axis decreases (e.g., Blandford and Rees 1978; Perley et al. 1980, 1982; Moore et al. 1981; Browne et al. 1982a,b; Orr and Browne 1982; Foley 1982; Wilkinson 1982; Bridle and Perley 1984; Bridle and Eilek 1985; Antonucci and Ulvestad 1985; Browne and Perley 1986; Browne 1987; Scheuer 1987).

In order to obtain more information on the radio properties of core-dominated sources, we have obtained high-resolution VLA observations of 16 core-dominated quasars and active galactic nuclei. The structure detected by our high-

resolution observations covers a wide range of source morphology. We detect isolated cores; one-sided jets; short, faint extensions to the cores, which may indicate the presence of jets; and single secondary components which may be hotspots or the brighter parts of lobes. Below, we discuss some of the implications of our observations for current unifying scenarios for core-dominated and lobe-dominated sources.

# II. OBSERVATIONS

#### a) The Sample

We selected 16 core-dominated sources based on two criteria: (1) They have a core-jet VLBI morphology; (2) Previous observations at lower resolution indicated that there was extended structure on scales of  $\gtrsim 1''$ .

These criteria were chosen to maximize the probability that a radio jet would be detected. Thus, the sample is biased and our results may not be safely extrapolated to other samples.

The source list is given in Table I. The source name (IAU designation) is given in column (1). An alternate name from the radio-source catalogs is given in column (2). The type of identification and redshift are given in columns (3) and (4). These are taken from the compilations of Véron-Cetty and Véron (1987) and Hewitt and Burbidge (1987). The scale factor in kpc/arcsec is given in column (5) assuming  $H_0 = 75 \text{ km s}^{-1} \text{ Mpc}^{-1}$  and  $q_0 = 0.0$ . A redshift of z = 1

<sup>&</sup>lt;sup>a)</sup> Current address: Radiosterrenwacht, Postbus 2, 7990 AA Dwingeloo, Netherlands.

b) Current address: Haystack Observatory, Westford, MA 01886.

c) The National Radio Astronomy Observatory (NRAO) is operated by Associated Universities, Inc., under contract with the National Science Foundation.

d) NRAO Summer Student.

Name	Alternate Name	ID	redshift	scale <sup>b</sup> kpc/arcsec
0224 + 671	4C 67.05	Q		7.3
0333 + 321	NRAO 140	Q	1.263	7.8
0605 - 085		Q	0.87	6.9
0735 + 178		BL Lac	>0.424	> 4.9
0836 + 710	4C 71.07	Q	2.16	8.7
0859 - 140	OJ-199	Q	1.327	7.9
1055 + 018	4C 01.28	Q	0.888	7.0
1116 + 128	4C 12.39	Q	2.118	8.7
1510 - 089		Q	0.361	4.5
1624 + 416	4C 41.32	BF <sup>a</sup>		7.3
1633 + 382	4C 38.41	Q	1.814	8.5
1642 + 690	4C 69.21	Q	0.751	6.5
1749 + 701		BL Lac		7.3
1807 + 698	3C 371	N Gal	0.051	0.9
1823 + 568	4C 56.27, OU539	Q	0.664	6.2
2037 + 511	3C 418	Q	1.687	8.4

<sup>&</sup>lt;sup>a</sup> Blank field. Peacock et al. (1981), Lebofsky et al. (1983).

(roughly the median value for the sample) is used for the three sources with unknown redshift.

## b) The First-Epoch VLA Observations

The sources were observed in the A configuration of the VLA (Thompson et al. 1980) on 8 March 1985. Observations at two adjacent frequencies with 50 MHz bandwidths were combined to obtain an effective bandwidth of 100 MHz at 4860 MHz (6.2 cm), 14 940 MHz (2 cm), and 22 460 MHz (1.3 cm), with typical resolutions of  $\sim 0.45, \sim 0.15$ , and  $\sim 0.08$ , respectively. Observations of 3C 84 were obtained over a wide range of parallactic angles and were used to calibrate the instrumental polarization. Observations of 3C 286 were used to place the data on the flux-density scale of Baars et al. (1977) and also to set the absolute polarization position angle. A tipping scan was obtained during the observing run and a correction for atmospheric extinction was applied to the observations at 1.3 cm. Each source was observed at each frequency twice in "snapshot" mode for a total of  $\sim 10$  min with the two snapshots taken  $\sim 2$  hr apart in order to improve the (u,v) coverage. The different frequencies were observed sequentially at each source, so both sets of multifrequency observations of each source were obtained within a period of a few hours. Sidelobes were removed using the CLEAN deconvolution algorithm (Clark 1980). The data were self-calibrated (Schwab 1980) using initially a point-source model and later a model composed of the non-negative CLEAN components. A correction was made for the Ricean bias in the polarized flux density (e.g., Killeen, Bicknell, and Ekers 1986).

#### c) The Second-Epoch VLA Observations

A subset of the sources exhibiting jets was reobserved on 6 May 1986 with longer integration times. 0605-085, 1510 - 089, 1642 + 690, and 1823 + 568 were observed at 6 cm, and 1823 + 568 and 2037 + 511 were observed at 2 cm. The sources were observed for  $\sim 2 \text{ hr}$  at 2 cm and  $\sim 1-1.5 \text{ hr}$ at 6 cm. The observations were calibrated and reduced as described above. The instrumental polarization was calibrated using observations of 1823 + 568. 3C 48 and 3C 138 were used to set the flux-density scale and absolute polarization position angle, respectively, for the observations of 0605 - 805.

Contour plots of total intensity with observed E vectors superposed (length proportional to fractional polarization) are shown in Figs. 1-19. Epoch 1950.0 coordinates are used. The ratio of the peak in the maps to the level of the lowest believable contour level is typically ~2000. In some cases, artifacts are present near the core in these maps. The E vectors are shown only where the 1  $\sigma$  error in position angle (based on the rms noise in the Stokes Q and U maps) is less than 10°. For transparent synchrotron emission (i.e., the extended structure), the projected (emissivity weighted) magnetic field should be perpendicular to the E vectors. The foreground Faraday rotation measures (RMs) for the extended structure are generally small (Simard-Normandin et al. 1981; Rudnick and Jones 1983; Wrobel et al. 1988), and thus the observed E vectors will be close to the intrinsic val-

Brief comments on the sources are given below. Unless we specifically mention structure at a given wavelength, the source is unresolved by our observations at that wavelength.

## III. RESULTS

# a) Core Parameters

The peak flux density, fractional polarization, and polarization position angle at the three wavelengths are given in Table II. The 22 485 MHz data are used for the core polar-

<sup>&</sup>lt;sup>b</sup> Assuming  $H_0 = 75 \text{ km s}^{-1} \text{ Mpc}^{-1}$  and  $q_0 = 0.0$ .

TABLE II. Core parameters.

NAME	Log <sub>10</sub> P <sub>6</sub> Watts/Hz	S <sub>6</sub> Jy	m <sub>6</sub> %	χ <sub>6</sub>	S <sub>2</sub> Jy	m <sub>2</sub> %	χ <sub>2</sub>	S <sub>1.3</sub> Jy	m <sub>1.3</sub> %	χ <sub>1.3</sub>	$ heta_{ m VLBI}$	Refs
0224+671	27.44	1.27	4.3	-85	1.36	2.0	-51	1.34	1.0	-36	-3	1
0333+321	27.87	2.07	5.1	60	1.11	6.7	41	0.97	5.4	35	130	1,2
0605-085	27.49	2.00	1.9	34	2.23	1.6	29	2.31	2.1	13	150	1
0735+178	>26.81	1.81	2.4	3	1.70	2.5	-19	1.60	3.1	-23	$60^a$	3
0836+710	28.44	2.22	9.1	-78	1.56	6.0	-74	1.69	4.4	-70	-143	4
0859-140	27.92	2.08	1.7	75	1.60	2.9	57	1.38	3.3	40	-6	1
1055+018	27.68	2.87	3.1	-61	4.41	5.3	-40	4.70	5.7	-42	-55	1
1116+128	28.24	1.47	3.2	-57	1.17	2.1	-58	1.15	1.4	-42	26	1
1510-089	26.60	1.54	3.1	46	2.18	1.3	7	2.23	2.2	-16	173	1
1624+416	27.41	1.19	< 0.1	•••	0.87	0.2	10	0.81	1.0	-13	69	5
1633+382	28.35	2.77	1.4	24	2.66	1.5	22	2.50	0.7	25	$-63^{b}$	5
1642+690	27.18	1.29	4.2	-65	1.53	10.6	-18	1.72	11.2	-12	-165	6
1749+701	27.51	1.50	5.0	85	1.15	5.6	83	1.16	6.3	85	-60	3
1807+698	24.86	1.45	3.6	<b>52</b>	1.66	2.8	-11	1.73	2.1	-21	-97	7
1823+568	27.05	1.25	5.0	37	1.63	7.2	19	1.68	8.0	15	-160	8
2037+511	28.29	2.80	1.3	76	2.64	1.3	57	2.38	2.2	67	-140	9
						Second	Epoch					
0605-085		2.30	1.2	61	•••	•••	•••	•••		•••		
1510-089	•••	1.48	2.5	60				•••	•••	•••		
1642+690	•••	1.37	4.0	-33	•••		•••	•••	•••	•••	•••	
1823 + 568	•••	1.16	6.0	29	1.27	8.5	9	•••		•••		
2037+511	•••	•••		•••	2.77	2.8	80	•••		•••	•••	

<sup>&</sup>lt;sup>a</sup> Uncertain because of curvature.

# References to VLBI Structure

1. Romney et al. (1984); Padrielli et al. (1986). 2. Marscher and Broderick (1985). 3. Bååth (1984). 4. Eckart et al. (1987); Witzel (1987). 5. Zensus et al. (1984). 6. Pearson et al. (1986). 7. Pearson and Readhead (1981); Lind (1987).

8. Lawrence (1985, private communication). 9. Neff and Muxlow (1987, private communication).

ization parameters at 1.3 cm because of problems with the 22 435 MHz data. The multifrequency data were taken within a period of a few hours and thus represent an instantaneous determination of the variable core properties. For the  $\sim$  1–2 Jy cores in this paper, the observational uncertainties are dominated by calibration and systematic errors rather than by signal-to-noise. The errors in the flux densities are due to the limited accuracy with which the absolute fluxdensity scale can be applied to the data and are  $\sim 2\%$ , 5%, and 10% at 6, 2, and 1.3 cm. Local variations (i.e., patchiness) in atmospheric attenuation (not corrected for with our tipping scan) dominate the uncertainty at 1.3 cm. The errors in fractional polarization are dominated by uncertainties in the calibration of the instrumental polarization and are  $\sim 0.1\%$  at the three wavelengths. The errors in absolute polarization position angle are  $\sim 2^{\circ}$  at 6 and 2 cm and  $\sim 4^{\circ}$  at 1.3 cm. Ionospheric Faraday rotation is unimportant at these short wavelengths.

The monochromatic power (W Hz<sup>-1</sup>) of the core at 6 cm in the rest frame of the source (assuming  $\alpha = 0.0$ ) is also

The position angle (measured positive east from north) of the orientation of the VLBI source (taken from the literature) is also given in Table II. Note that unless the location of the flat-spectrum core is known, there will be a 180° ambiguity in the VLBI position angle.

# b) Parameters of the Extended Emission

Some parameters of the extended emission are given in Table III. The source name is given in column (1). The monochromatic power at 21 cm in the rest frame of the source (assuming  $\alpha = -0.75$ ) is given in column (2). The flux density of the extended emission at 6 cm is given in column (3). We compared our measurements of the flux density of the extended structure with previous lower-resolution measurements in the literature, when these were available. In a few cases, our observations resolve out a significant fraction of the flux density and we used the previous measurements (references are given in the footnotes to the table). A spectral index of  $\alpha = -0.75$  was used to extrapolate the flux density from data at other frequencies. The ratio between the surface brightnesses of the two sides of the source (at similar distances from the core) is given in column (4). For the one-sided sources, the ratio of the peak brightness of the observed emission to the  $3\sigma$  upper limit to

<sup>&</sup>lt;sup>b</sup> Kellermann et al. (1977) give pa  $\sim 165^{\circ}$ .

TABLE III. Parameters of the extended emission.

NAME	$\begin{array}{c} \text{Log}_{10} \text{ P}_{21} \\ \text{Watts Hz}^{-1} \end{array}$	S <sub>6</sub> mJy	side-to-side asymmetry	$\beta\cos\theta$	PA at 1"	Δ PA <b>•</b>	LAS	LLS kpc	$P_{minP}$ (×10 <sup>-10</sup> ) dynes cm <sup>-2</sup>	${ m B_{minP}} \ \mu { m G}$
0224+671	26.87	80	7	0.34	0/180	145	30°	220	0.6	25
0333+321	26.70	30	2.5	0.17	150	0	8	62	0.7	28
0605-085	26.70	80	9	0.38	93	30	5.5	38	3	58
0735+178	>25.67	40	3	0.20	177	45	2	10	3	54
0836+710	27.72	70	43	0.60	-160	0	2	17	20	150
0859-140	26.76	30	2.5	0.17	162	Õ	12e	95	3	54
1055+018	26.68	70ª	10°	0.40	180ª	20	$30^a$	210	0.6	25
1116+128	27.96	130	58	0.63	-33	70	3	26	30	170
1510-089	25.99	120	5	0.29	160	20	9	40	2	43
1624+416	26.44	30	21	0.50	-11	40	1	7	10	100
1633+382	26.65	10°	10ª	0.40	180°	60	$12^a$	100	0.9	31
1642+690	26.77	130	45	0.60	-174	40	10	65	4	65
1749+701	25.96	10	3	0.20	-150	0	0.4	3	35	190
1807+698	24.72	$40^{b,c}$	20	0.50	-125	20	$290^d$	260	6	82
1823+568	26.76	170	104	0.69	173	180	15ª	93	7	84
2037+511	28.12	360	46	0.60	-28	125	3	25	23	160

<sup>&</sup>lt;sup>a</sup> Murphy (1988).

the surface brightness of any possible counter component is given. The constraint on  $\beta$  cos  $\theta$  from Eq. (2) assuming the source is intrinsically symmetric is given in column (5). The position angle of the emission 1" from the core is given in column (6). The misalignment between the structure closest to and furthest from the core seen in the VLA images is given in column (7). The total angular extent of the source (largest angular size, LAS) is given in column (8). The projected size in kiloparsecs (using the scale factor given in Table I) is given in column (9). The minimum pressure in the extended emission and the magnetic field corresponding to minimum pressure (e.g., Burns, Owen, and Rudnick 1979; O'Dea and Owen 1987) are given in columns (10) and (11), respectively. We adopt a filling factor of unity, a ratio of energy in relativistic electrons to other particles of unity, and upper and lower frequency limits of 10<sup>11</sup> and 10<sup>7</sup> Hz, respectively, and assume cylindrical symmetry for the extended structure. Note that if the flux density of the extended emission has been Doppler boosted, the power and the minimum pressure and corresponding magnetic field will be overestimated.

#### IV. INDIVIDUAL SOURCE DESCRIPTIONS

0224+671. Perley, Fomalont, and Johnston (1980, 1982, hereafter referred to as PFJ80 and PFJ82) present VLA maps at 20 cm which show triple structure in this source. Our 6 cm observations resolve out all the extended structure except for a diffuse component (angular distance from the core  $\theta_d \simeq 7''$ , position angle (P.A.)  $\simeq -178^\circ$ ) coincident with the peak of the southern component seen by PFJ80 and PFJ82.

0333 + 321. Schilizzi and de Bruyn (1983) detect both the SE component and a weaker (by a factor of  $\sim 3$ ) NW com-

ponent with their 6 cm WSRT observations. Our 6 cm VLA observations detect only the SE component ( $\theta_d \approx 7$ ".6, P.A.  $\approx 150^\circ$ ), consistent with previous observations (Browne et al. 1982b; Perley 1982; Browne 1987). EVN observations at 1.66 and 5 GHz show that the core is elongated at P.A.  $\sim 135^\circ$  (Pilbratt, Booth, and Porcas 1987), in good agreement with the VLBI P.A.  $\sim 130^\circ$  (Marscher and Broderick 1985) but misaligned by  $\sim 15^\circ$  with the P.A. of the SE arcsecond-scale component.

0605 – 085 (Fig. 1, 6 cm). At 6 cm; we have detected a jet of length  $\theta_1 \simeq 5''$  which starts out at P.A.  $\simeq 93^\circ$  and then bends by  $\simeq 30^\circ$  to the southeast. The inferred direction of the magnetic field is initially parallel to the local jet axis, is unknown in the middle of the jet, and is perpendicular to the local axis at the end of the jet.

0735+178 (Fig. 2, 6 cm; Fig. 3, 2 cm). Using low-resolution (~40") 20 cm VLA observations, Ulvestad and Johnston (1984) place an upper limit of  $\sim 2$  mJy to the flux density of any extended structure on scales of > 10".20 cm VLA observations with a resolution of  $\sim 1.2$  by Murphy (1988) show an extension of length  $\theta_1 \simeq 2''$  south of the core. At 6 cm, we detect a jet with length  $\theta_1 \sim 2''$  which starts at  $P.A. \sim 180^{\circ}$  and curves to the SW near its visible tip. The "ear" on the core to the west is most likely spurious. Polarization is detected at only a few points along the jet. The position angle is consistent with a magnetic field that is parallel to the jet axis. At 2 cm, we also detect a short curved jet extending  $\theta_1 \sim 0.4$  south of the core. The VLBI jet apparently starts out at an angle of  $\sim 60^{\circ}$  and bends to the southeast (Bååth 1984). Thus, there is considerable curvature of the jet between the 1 mas and 100 mas size scales.

**0836+710** (Fig. 4, 6 cm). We detect a secondary component at distance  $\theta_d \simeq 1^{"}5$  and P.A.  $\simeq -162^{\circ}$  consistent with

<sup>&</sup>lt;sup>b</sup> Antonucci and Ulvestad (1985).

<sup>&</sup>lt;sup>c</sup> Perley et al. (1982).

<sup>&</sup>lt;sup>d</sup> Ulvestad and Johnston (1984).

<sup>&</sup>lt;sup>e</sup> Perley (1982).

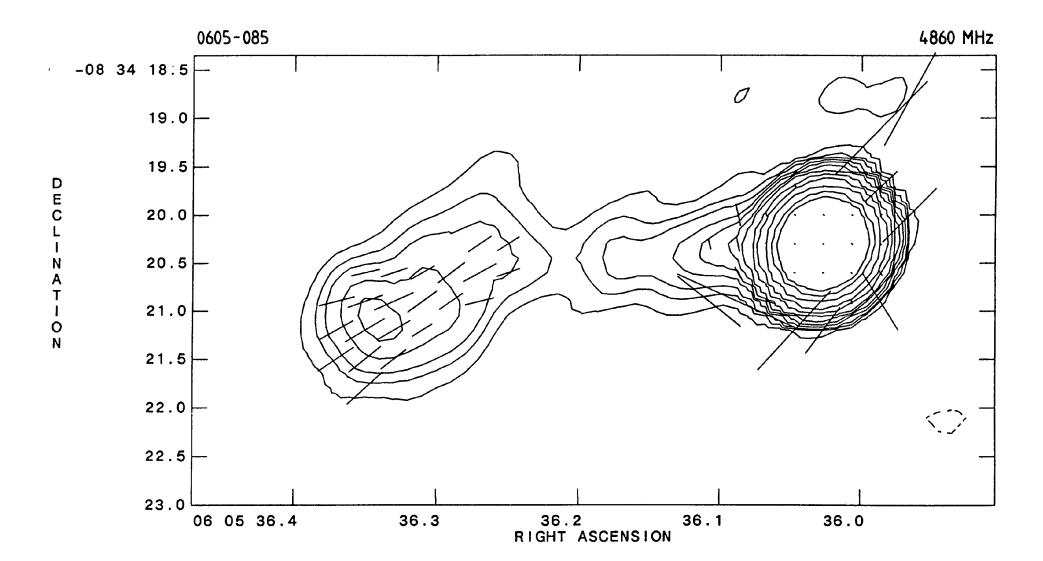


Fig. 1. 0605-085. Contour plot of total intensity at 6 cm with E vectors superposed whose length is proportional to the fractional polarization. 1 arcsec = 67%. Contour levels are -1 (dashed), 1, 2, 3, 5, 7, 10, 15, 30, 50, 100, 200, and 300 mJy per beam. The clean-beam FWHM is  $0.57 \times 0.54$  at -40°.

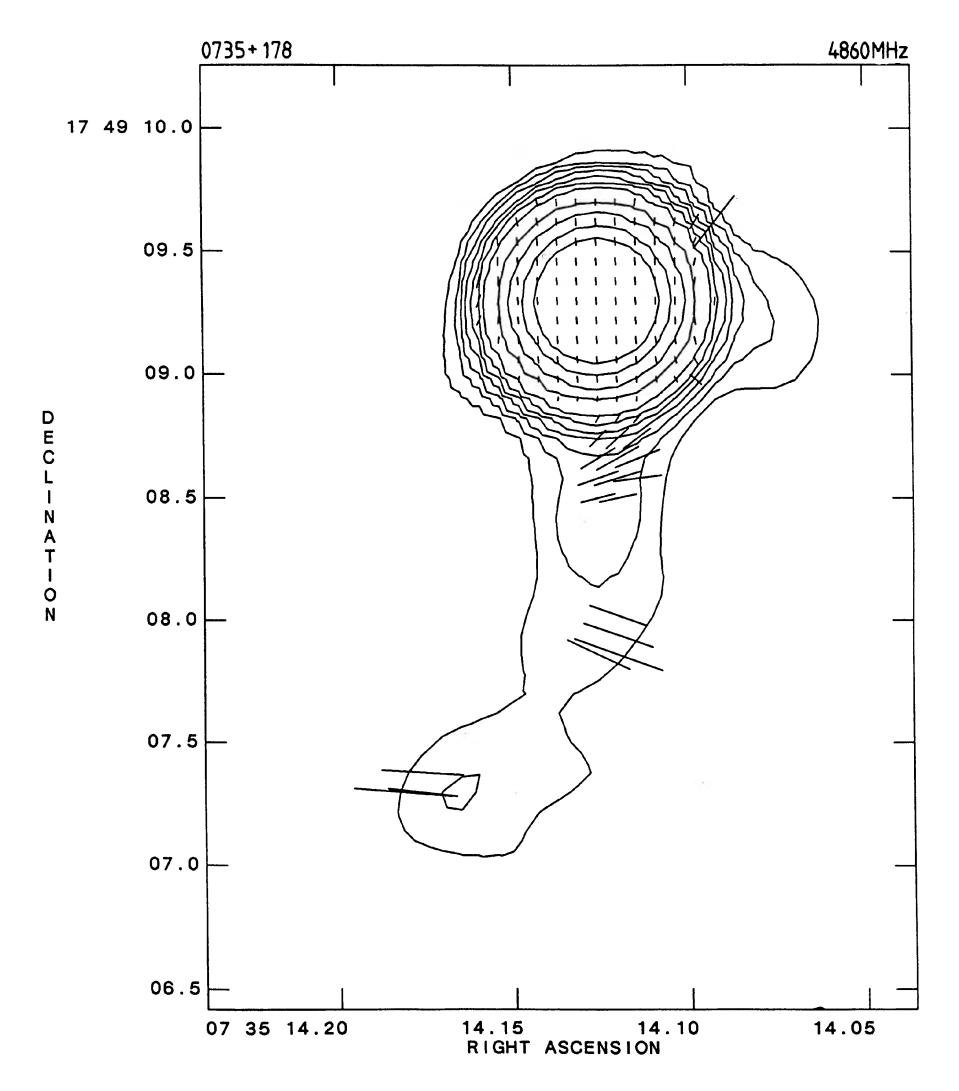


FIG. 2. 0735 + 178. Contour plot of total intensity at 6 cm with E vectors superposed whose length is proportional to the fractional polarization. 1 arcsec = 83%. Contour levels are - 1.5 (dashed), 1.5, 3, 5, 8, 12, 18, 30, 75, 150, 300, and 500 mJy per beam. The clean-beam FWHM is 0"37.

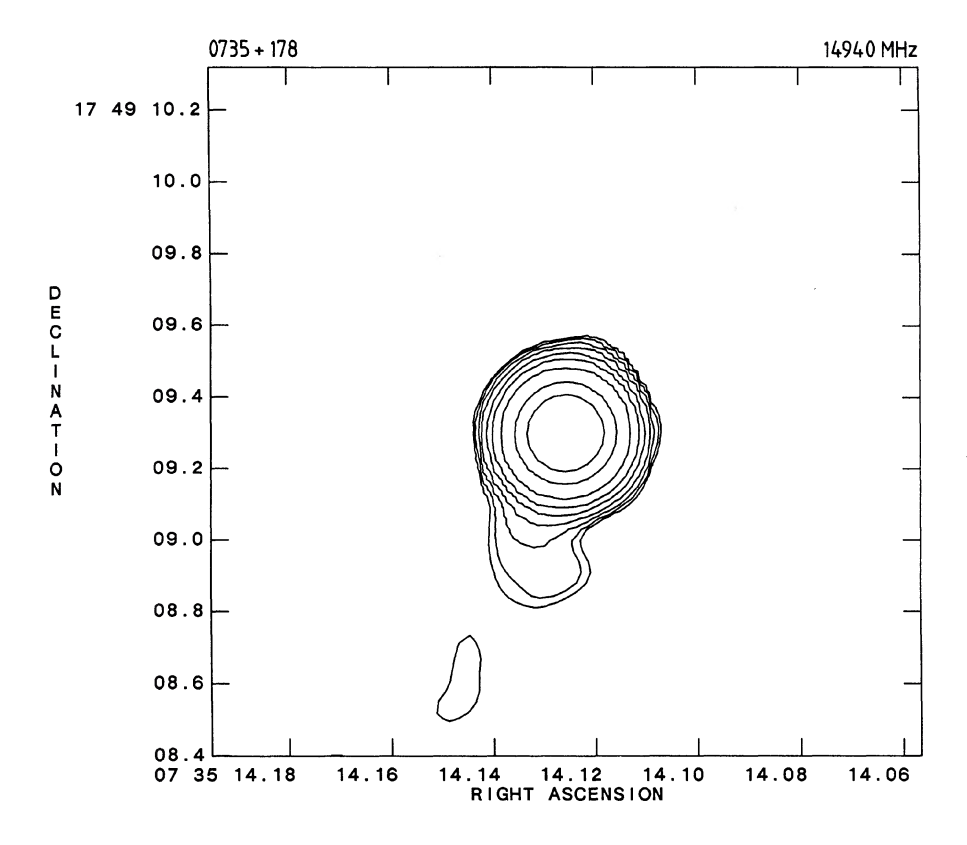


Fig. 3. 0735 + 178. Contour plot of total intensity at 2 cm. Contour levels are -1.5 (dashed), 1.5, 2, 3, 5, 10, 20, 50, 200, and 500 mJy per beam. The clean-beam FWHM is 0"16.

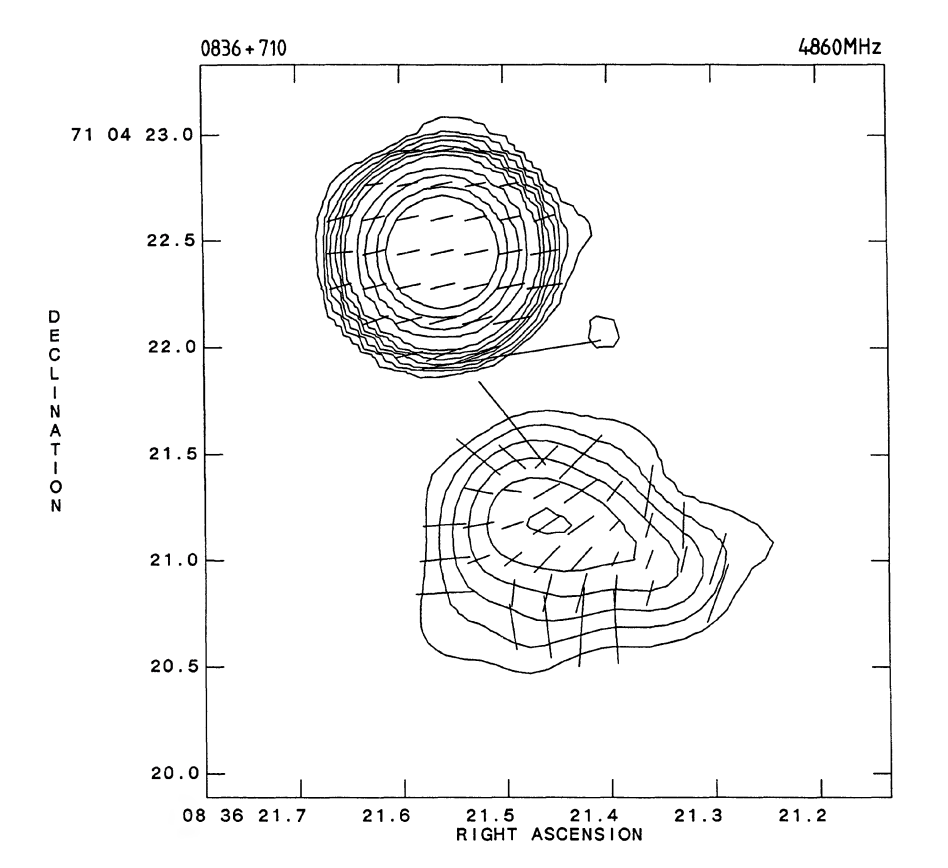


FIG. 4. 0836 + 710. Contour plot of total intensity at 6 cm with E vectors superposed whose length is proportional to the fractional polarization. 1 arcsec = 83%. Contour levels are -1.5 (dashed), 1.5, 3, 5, 8, 12, 18, 30, 75, 150, 300, and 500 mJy per beam. The clean-beam FWHM is 0.36

previous VLA observations (PFJ80; Perley 1982). The magnetic field in the secondary component appears to be circumferential.

**0859**—**140.** Perley (1982) reports that the source is a triple with total extent  $\theta_{LAS} \sim 12''$ . At both 6 and 2 cm, we detect a weak extension to the core in the direction of a diffuse secondary component detected at 6 cm at  $\theta_d \simeq 6''$  in P.A.  $\simeq 162^\circ$ .

1055+018. 20 cm VLA observations by Murphy (1988) show a triple source with total extent of  $\theta_{LAS} \sim 30''$  with a jet extending south of the core. Perley (1982) also detects a secondary component to the south. Our 6 cm VLA observations resolve out all structures except the core.

1116+128 (Fig. 5, 6 cm; Fig. 6, 2 cm; Fig. 7, 1.3 cm). Perley (1982) detected a secondary component at  $\theta_d \sim 2$ . 5 at P. A.  $\sim 315^\circ$ . Our 6 cm VLA data show diffuse emission to the east of the secondary component (a hotspot?). The "jet-like" extension to the core (seen both at 6 and 2 cm) points towards the more diffuse emission to the northeast of the secondary component. The magnetic field in the secondary component is parallel to the direction to the core.

The 2 and 1.3 cm data show that the jet extends from the core initially at  $P.A. \approx 13^{\circ}$  and then curves gradually by  $\sim 55^{\circ}$  to point at the lobe in the 6 cm map.

1510–089 (Fig. 8, 6 cm; Fig. 9, 2 cm; Fig. 10, 1.3 cm). At 20 cm, Perley (1982) detects a one-sided jet with length  $\theta_1 \approx 8''$  at P.A.  $\approx 160^\circ$ . In our 6 cm image of the jet, the polarization is undetected over the middle part of the jet, but is consistent with a magnetic field that is parallel to the jet axis until the end of the jet, where it becomes perpendicular. The magnetic field also flips to a roughly perpendicular orientation at the locations of two knots in the jet. The two "ears" seen on the core in the 6 cm image are spurious.

At both 2 and 1.3 cm (Figs. 9 and 10), we detect a slightly resolved (deconvolved size at 1.3 cm is  $0.1 \times 0.07$ ) secondary component with an integrated flux density at 1.3 cm of  $S \sim 26$  mJy and an integrated spectral index between 1.3 and 2 cm of  $\alpha \sim -0.6$ . The component is at  $\theta_d \simeq 0.07$ 3 at  $P.A. \simeq -28^\circ$ , which is approximately 180° from the inner part of the jet (at  $P.A. \simeq 155^\circ$ ). Thus, it is likely that this component is part of a counterjet. At 2 cm, the E vector of this component is roughly aligned with the direction to the core. Thus, if the RM is small, the magnetic field is perpendicular to the counterjet, as found in many knots and hotspots (e.g., Dreher 1981; Bridle 1984; Bridle and Perley 1984).

Until additional structure on the counterjet side is detected, it will not be known whether this counter component represents a knot near the base of a counterjet or a hotspot at the end of the counterjet. If the component is indeed a terminal hotspot, and the two sides of the source were ejected symmetrically from the nucleus, then a constraint on the hotspot-advance speed is obtained, assuming that the difference in lengths of the two sides of the source is due to relative light-travel times (e.g., Longair and Riley 1979). Under this hypothesis, the observed ratio of the lengths of the two sides give an inferred hotspot-advance speed of  $\beta$  cos  $\theta \sim 0.93$ .

1624+416 (Fig. 11, 6 cm). This source is a blank field in the optical (Peacock et al. 1981) but has been detected in the infrared K band (Lebofsky, Rieke, and Walsh 1983). We note that at 6 and 2 cm this source has the lowest fractional polarization in the core of any of the sources studied here. Perley (1982) reports a single secondary component at distance  $\theta \sim 0.77$  at P.A.  $\sim 352^\circ$ . Our 6 cm observations detect an extension to the core at P.A.  $\sim 345^\circ$  with length  $\sim 1.1^\circ$ . The magnetic field is parallel to the axis of the extension. Our 2

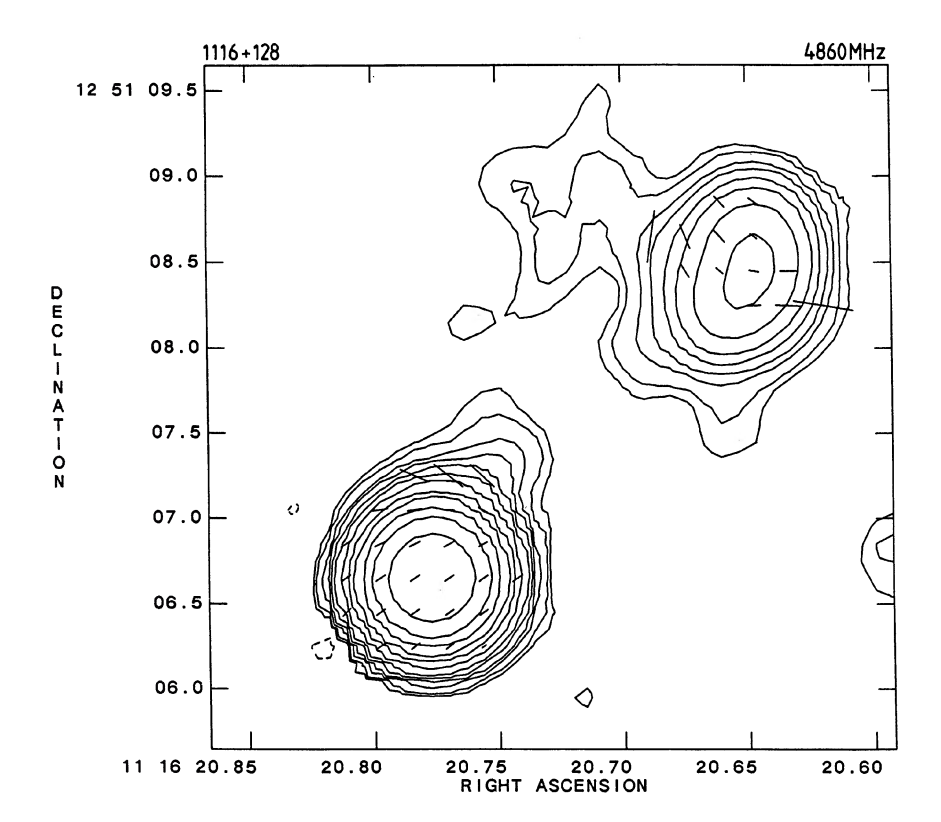


Fig. 5. 1116 + 128. Contour plot of total intensity at 6 cm with E vectors superposed whose length is proportional to the fractional polarization. 1 arcsec = 50%. Contour levels are -0.6 (dashed), 0.6, 1, 2, 3, 5, 8, 15, 30, 50, 100, 200, and 500 mJy per beam. The clean-beam FWHM is  $0^{\prime\prime}40$ .

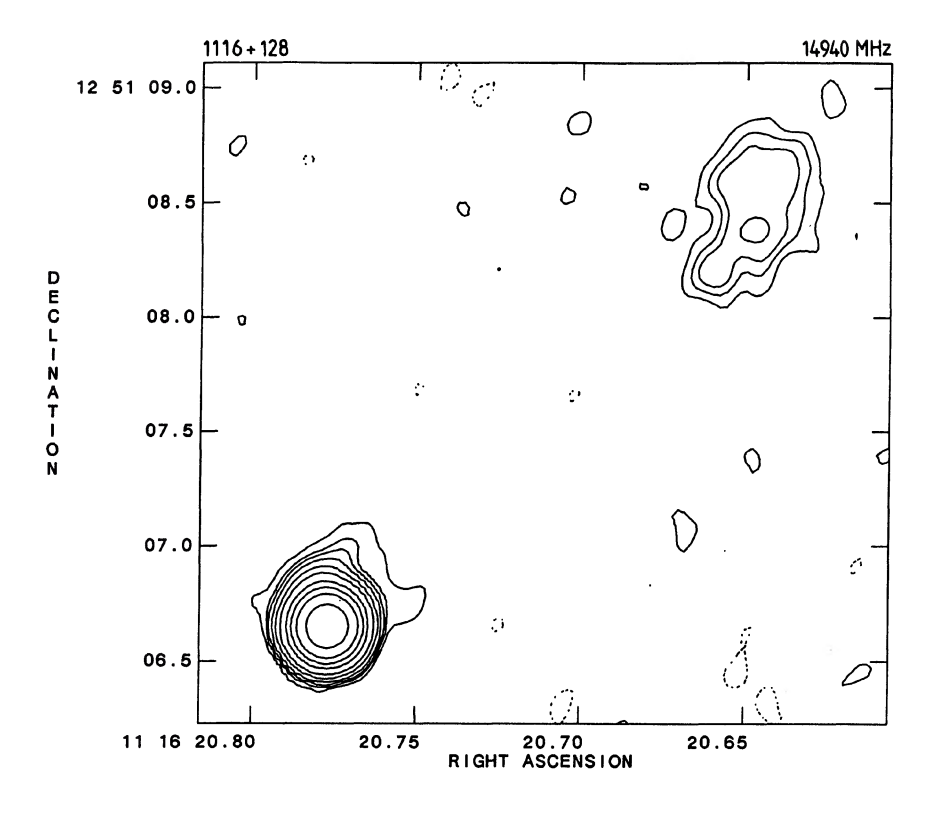


Fig. 6. 1116+128. Contour plot of total intensity at 2 cm. Contour levels are -1 (dashed), 1, 2, 3, 5, 10, 20, 50, 100, 200, and 500 mJy per beam. The clean-beam FWHM is 0.17.

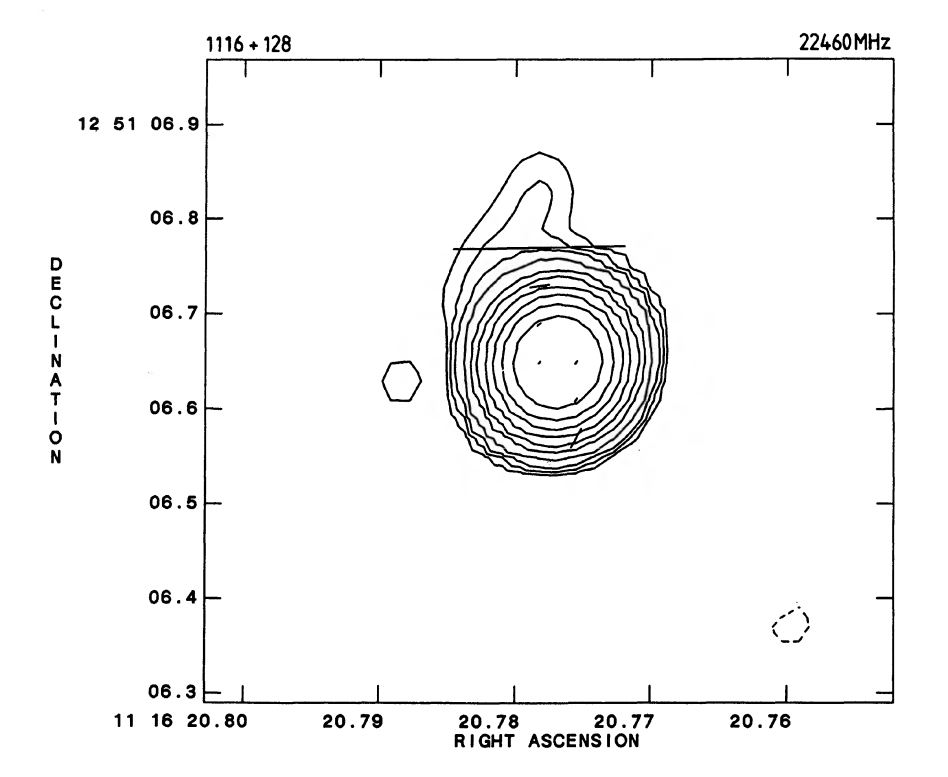


Fig. 7. 1116+128. Contour plot of total intensity at 1.3 cm with E vectors superposed whose length is proportional to the fractional polarization. 1 arcsec = 250%. Contour levels are -6 (dashed), 6, 10, 15, 25, 50, 75, 125, 200, 300, and 500 mJy per beam. The clean-beam FWHM is 0"087.

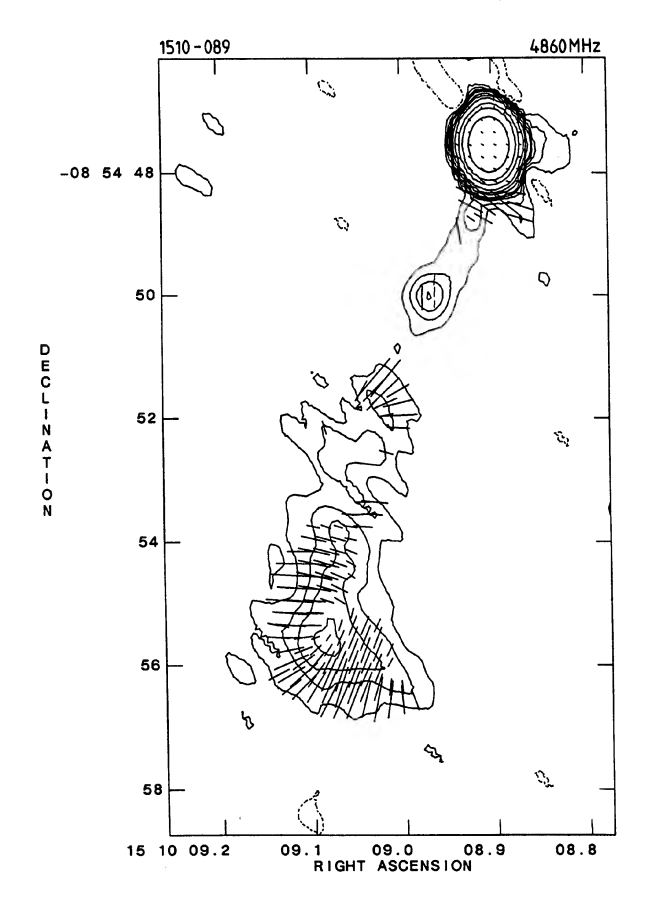


FIG. 8. 1510 - 089. Contour plot of total intensity at 6 cm with E vectors superposed whose length is proportional to the fractional polarization. 1 arcsec = 67%. Contour levels are - 1 (dashed), 1, 2, 3, 4, 5, 8, 12, 20, 50, 100, and 300 mJy per beam. The clean-beam FWHM is 0".59 $\times$ 0".42 at 3°.

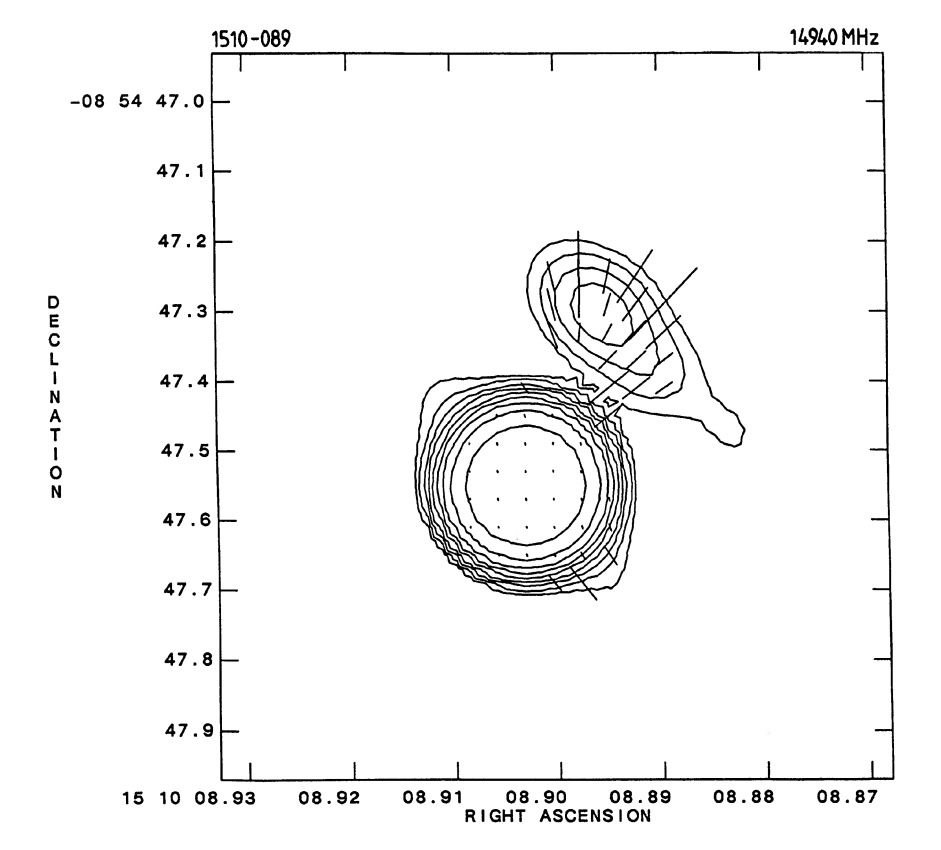


FIG. 9. 1510-089. Contour plot of total intensity at 2 cm with E vectors superposed whose length is proportional to the fractional polarization. 1 arcsec = 500%. Contour levels are -3 (dashed), 3, 5, 8, 12, 20, 30, 50, 100, and 300 mJy per beam. The clean-beam FWHM is 0''10.

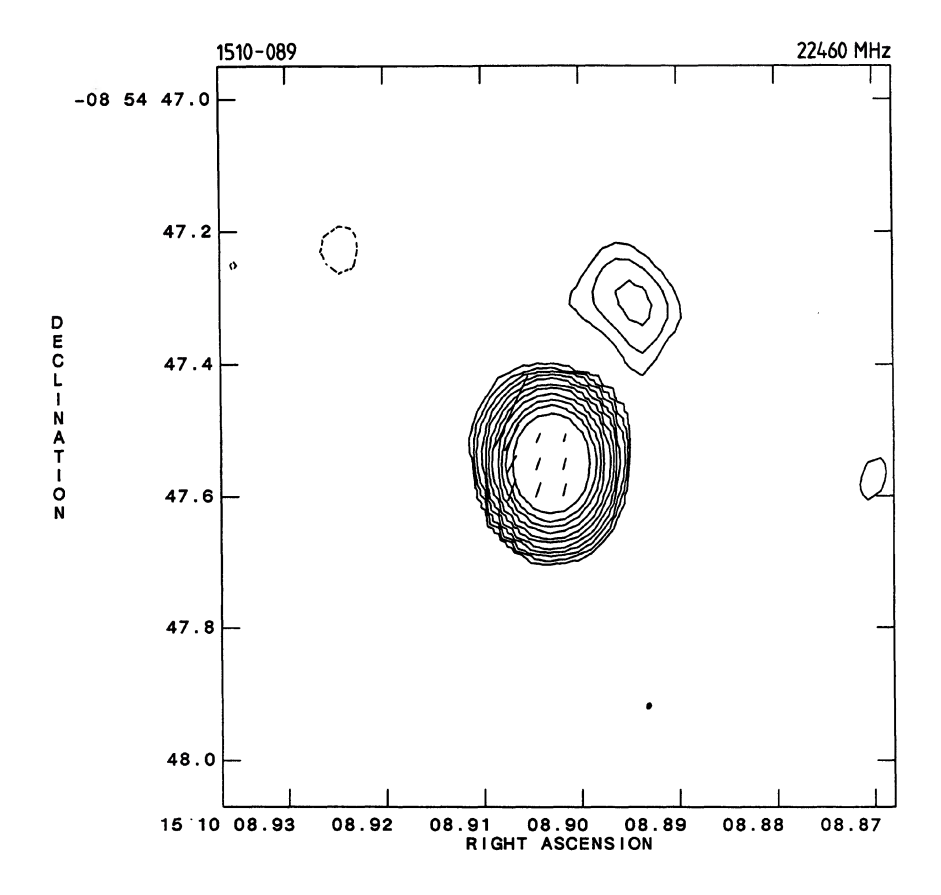


Fig. 10. 1510 - 089. Contour plot of total intensity at 1.3 cm with E vectors superposed whose length is proportional to the fractional polarization. 1 arcsec = 70%. Contour levels are - 5 (dashed), 5, 8, 12, 20, 30, 50, 75, 125, 200, 300, and 500 mJy per beam. The clean-beam FWHM is 0".10 $\times$ 0".08 at 2°.

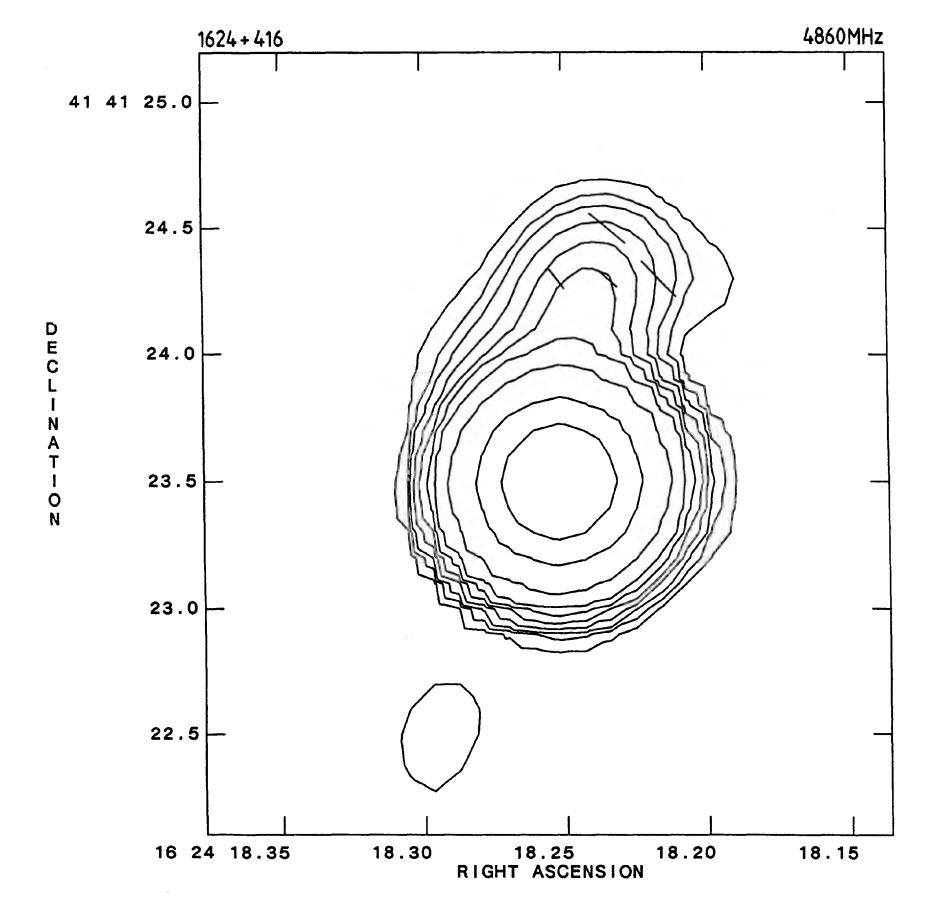


Fig. 11. 1624 + 416. Contour plot of total intensity at 6 cm with E vectors superposed whose length is proportional to the fractional polarization. 1 arcsec = 67%. Contour levels are -1 (dashed), 1, 2, 3, 5, 8, 12, 20, 50, 200, and 500 mJy per beam. The clean-beam FWHM is 0".40.

cm observations show a secondary component with a peak of 2 mJy at  $\sim$  0".5 from the core coincident with the 6 cm extension.

**1633+382.** Murphy (1988) reports a triple source with total extent  $\theta_{LAS} \sim 12''$ . Our observations resolve out all the extended structure.

1642+690 (Fig. 12, 6 cm). The source was recently discovered to be superluminal (Pearson et al. 1986). The source has a jet to the south extending  $\sim 4''$  from the core and a lobe to the north at a distance of  $\sim 6''$  (Browne et al. 1982a; Perley, Fomalont, and Johnston 1980; Browne and Orr 1981; Perley 1982; Rusk and Rusk 1986; Murphy 1988). The 20 cm data also show additional diffuse emission around the jet (Rusk and Rusk 1986; Browne 1987; Murphy 1988). Our 6 cm observations show both the southern jet and the northern hotspot in the lobe. The source has a "C" distortion and the angle at the core subtended by the two ends of the source is  $\sim 150^\circ$ . The magnetic field is parallel to the jet axis until roughly halfway down the jet and is perpendicular to

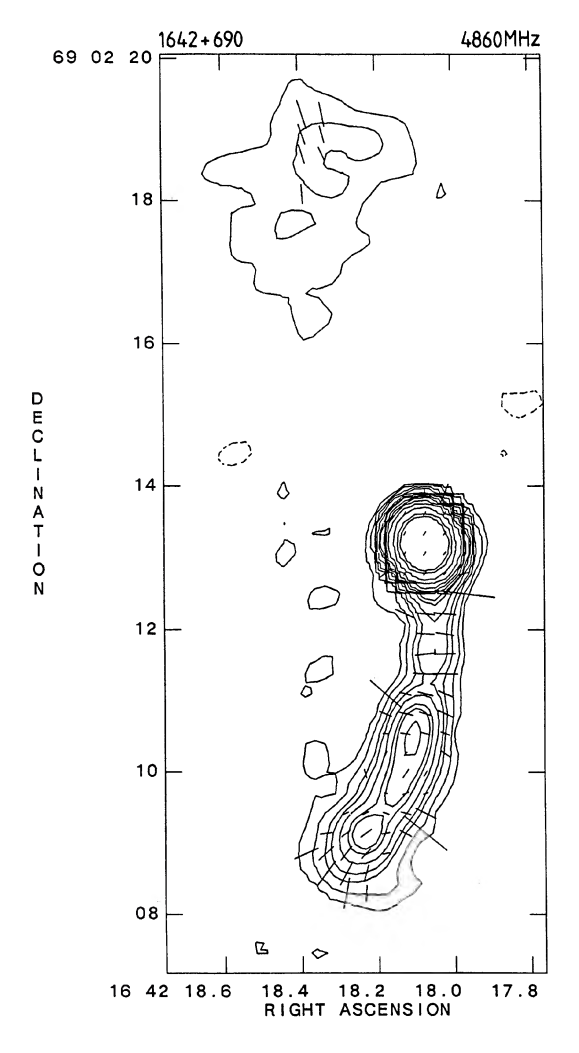


Fig. 12. 1642 + 690. Contour plot of total intensity at 6 cm with E vectors superposed whose length is proportional to the fractional polarization. 1 arcsec = 71%. Contour levels are -0.5 (dashed), 0.5, 1, 2, 3, 5, 8, 10, 15, 20, 30, 50, 100, 200, and 300 mJy per beam. The clean-beam FWHM is  $0.51 \times 0.44$  at 1.9°.

the jet axis thereafter. The transition takes place at the position of the bright knot in the middle of the jet. This transition is a counterexample to the trend in powerful sources for the magnetic field to be parallel to the jet axis for the entire length of the jet (Bridle 1984).

1749 + 701. (Fig. 13, 2 cm) Perley (1982) reports a halo of size 0".4 at 6 cm surrounding the core. At 2 cm, we detect a secondary component of flux density  $S \simeq 5.2$  mJy at  $\theta_d \simeq 0$ ".4 and P.A.  $\simeq -150^\circ$ .

1807+698 (Fig. 14, 6 cm; Fig. 15, 2 cm). The arcsecond scale structure consists of a jet of length  $\theta_1 \simeq 3''$  at P.A.  $\simeq -116^\circ$  which connects with a secondary component "A," plus a second component "B" at 40" from the core (Perley, Fomalont, and Johnston 1980; Browne *et al.* 1982a; Pearson, Perley, and Readhead 1985; Wrobel 1987). The large-scale structure consists of a diffuse component  $\sim 4'.8$  ( $\sim 27$  kpc for  $H_0 = 75$ ) in total extent at P.A.  $\sim 95^\circ$ , roughly symmetric with respect to the core (Ulvestad and Johnston 1984). Our 6 cm polarization data show that the magnetic field is parallel to the axis of the 3" jet. Our 2 cm data show that component A has a fairly flat "L-shaped" plateau.

1823 + 568 (Fig. 16, 6 cm; Fig. 17, 2 cm). Our data show a jet initially extending south from the core and then curving to the east and wiggling (consistent with Foley's 18 cm MERLIN map (Foley 1982; Wilkinson 1982)). The lower-resolution 20 cm maps of Murphy (1988) and Wrobel (1987, private communication) show diffuse emission on both sides of the source, though mainly concentrated to the western side of the core. The 408 MHz MERLIN map (Foley 1982) suggests the existence of a component to the west of the core.

2037+511 (Fig. 18, 6 cm; Fig. 19, 2 cm). Muxlow et al. (1984) present 18 cm MERLIN and combined EVN/MERLIN maps of this extremely curved jet. We detect similar structure at 2 cm. The 6 cm image shows a component located at  $\theta_d \simeq 3''$  to the north of the core whose relationship to the source is unclear. The inferred projected magnetic field orientation is parallel to the axis of the jet except at brightness enhancements (knots).

#### V. DISCUSSION

a) The Alignment of the Inferred Magnetic Field in the Core with the VLBI Jets

Figure 20 shows histograms of the difference between the polarization position angle (E vector) of the core at 6, 2, and 1.3 cm and the orientation of the VLBI jet (from Table II). There is only a slight preference for the E vectors to be perpendicular to the VLBI orientation at 6 cm. There is even less preference at 2 cm, and at 1.3 cm the distribution is completely random. This is in contrast to the strong trend for the inferred B field in the core to be aligned with the VLBI jet found by Rusk and Seaquist (1985) and Jones et al. (1985). We consider three possibilities for the discrepancy.

Most of these core-dominated sources are known to be variable (e.g., Aller et al. 1985; Rudnick et al. 1985). One possibility is that variability in the cores has introduced a large amount of scatter in our histograms. There might be less scatter in the Rusk and Seaquist and Jones et al. histograms since they averaged or took median values of position angles measured at several epochs. The wavelength dependence of the scatter (Fig. 20) would require that the variability is a very strong function of wavelength. Some wavelength dependence of the amplitude of polarization variability is

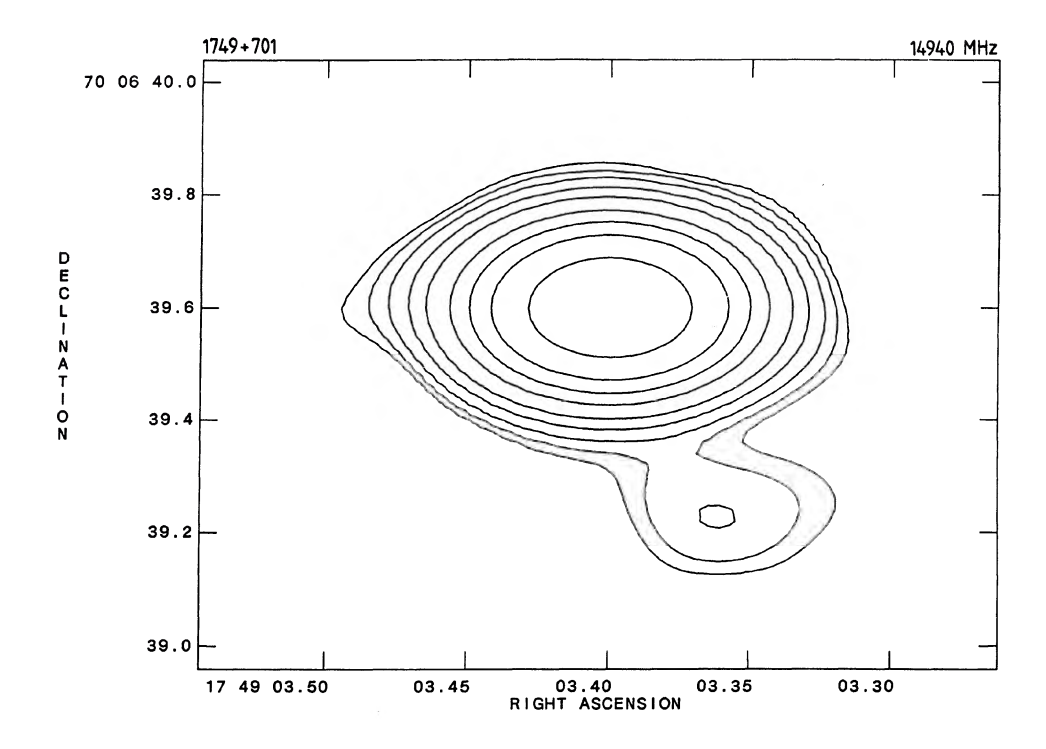


FIG. 13. 1749 + 701. Contour plot of total intensity at 2 cm. Contour levels are -2 (dashed), 2, 3, 5, 10, 20, 50, 100, 200, and 500 mJy per beam. The clean-beam FWHM is  $0.27 \times 0.16$  at  $90^\circ$ .

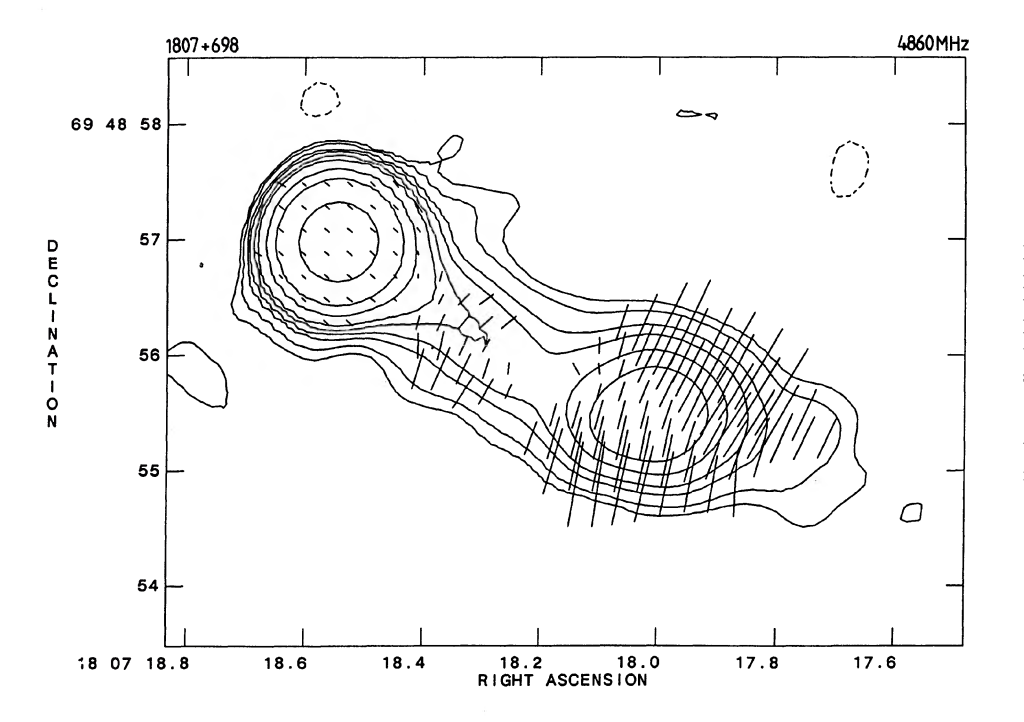


FIG. 14. 1807 + 698. Contour plot of total intensity at 6 cm with E vectors superposed whose length is proportional to the fractional polarization. 1 arcsec = 67%. Contour levels are - 1.2 (dashed), 1.2, 2, 4, 6, 10, 15, 40, 100, and 500 mJy per beam. The clean-beam FWHM is 0.55.

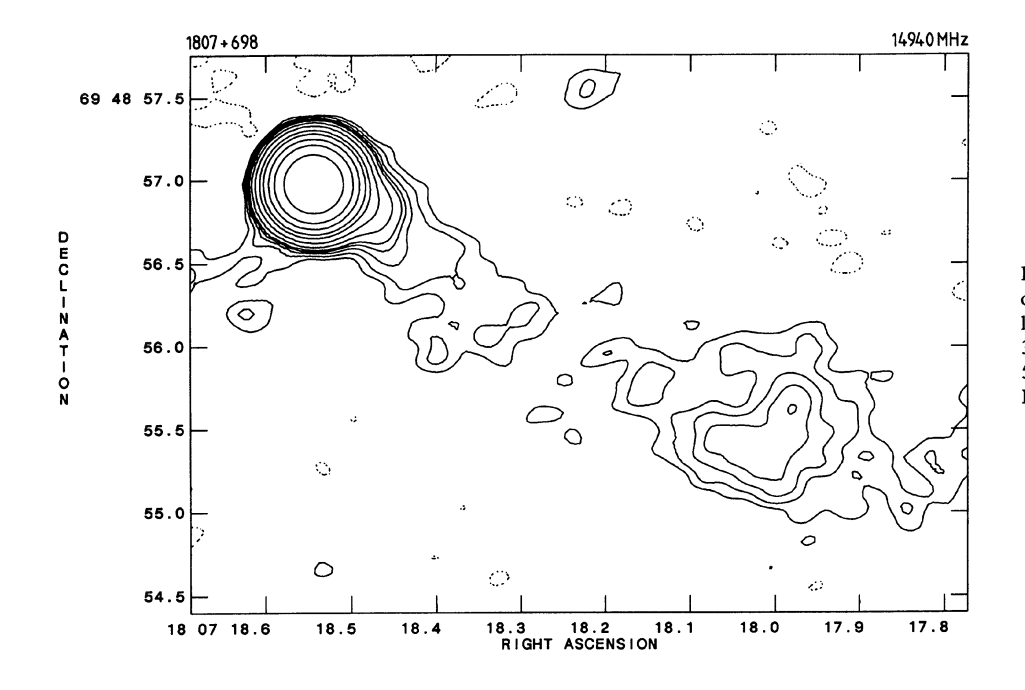


FIG. 15. 1807+698. Contour plot of total intensity at 2 cm. Contour levels are -1.2 (dashed), 1.2, 2, 3, 4, 5, 8, 15, 30, 50, 100, 200, and  $500\,\mathrm{mJy}$  per beam. The clean-beam FWHM is 0''.27.

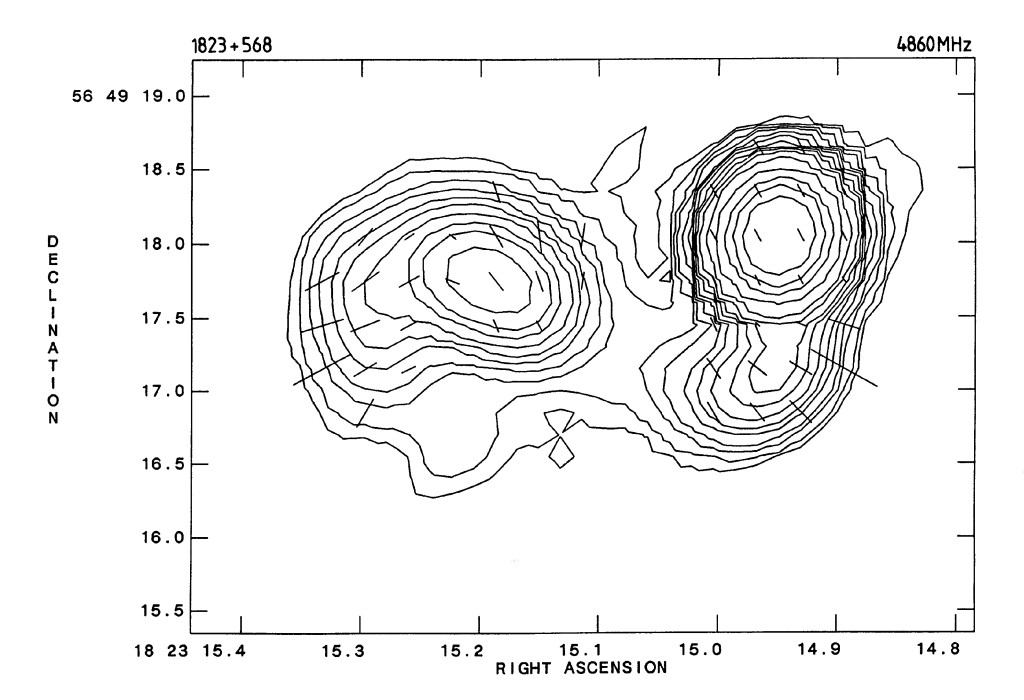


FIG. 16. 1823 + 568. Contour plot of total intensity at 6 cm with E vectors superposed whose length is proportional to the fractional polarization. 1 arcsec = 67%. Contour levels are -0.6 (dashed), 0.6, 1, 2, 3, 5, 7, 10, 15, 20, 30, 50, 100, 200, 300, and 500 mJy per beam. The clean-beam FWHM is  $0.47 \times 0.49$  is  $0.49 \times 0.4$ 

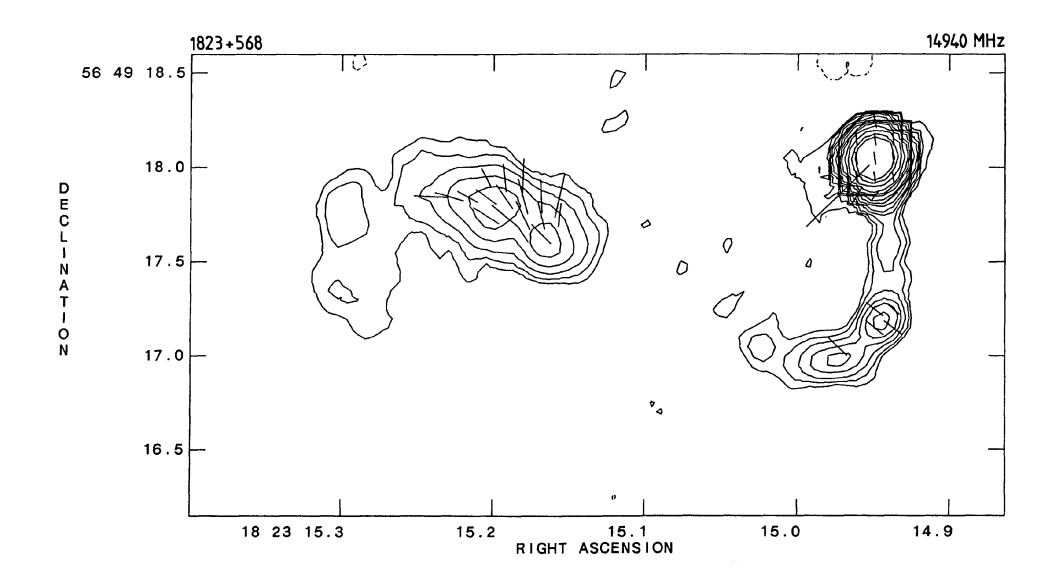


FIG. 17. 1823 + 568. Contour plot of total intensity at 2 cm with E vectors superposed whose length is proportional to the fractional polarization. 1 arcsec = 133%. Contour levels are -0.4 (dashed), 0.4, 0.7, 1.2, 2, 3, 5, 8, 12, 20, 30, 50, 100, 200, and 300 mJy per beam. The clean-beam FWHM is  $0.15 \times 0.14$  at -20.14.

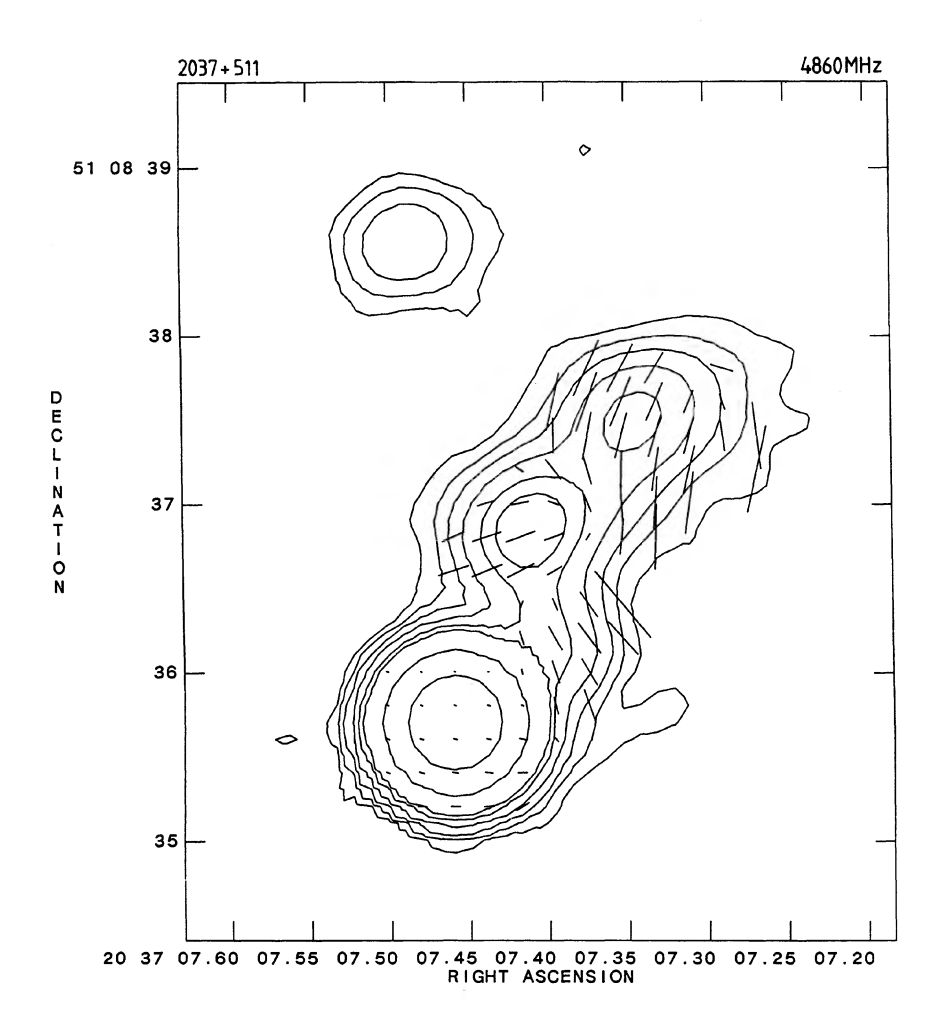


Fig. 18. 2037 + 511. Contour plot of total intensity at 6 cm with E vectors superposed whose length is proportional to the fractional polarization. 1 arcsec = 67%. Contour levels are -2 (dashed), 2, 5, 10, 20, 40, 60, 250, and 1000 mJy per beam. The clean-beam FWHM is 0".45.

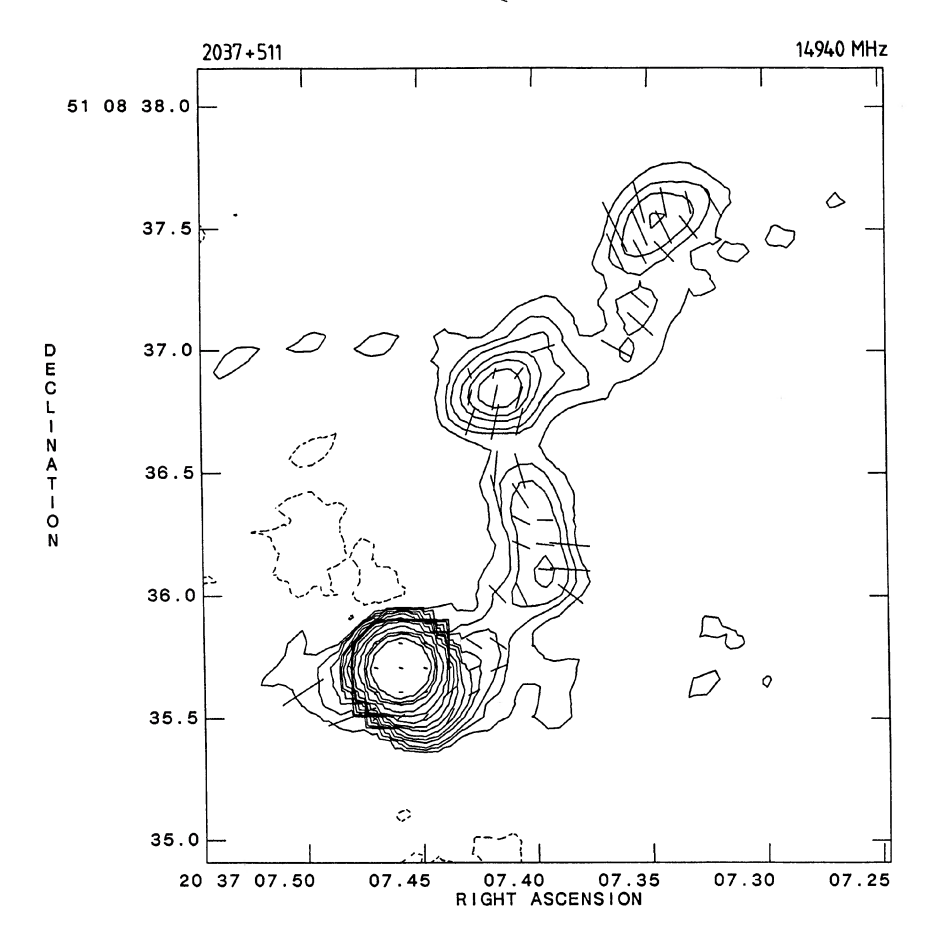


FIG. 19. 2037 + 511. Contour plot of total intensity at 2 cm with **E** vectors superposed whose length is proportional to the fractional polarization. 1 arcsec = 200%. Contour levels are -1 (dashed), 1, 2, 3, 5, 7, 10, 15, 20, 30, 50, 100, 200, 300, and 500 mJy per beam. The clean-beam FWHM is 0°15.

indeed observed (e.g., Aller *et al.* 1985). Thus, wavelength-dependent variability may explain at least part of the discrepancy.

A second possibility is that the lower-resolution measurements used by previous workers are contaminated by emission on the arcsecond and/or subarcsecond scales which is blended with the core in their measurements but is resolved out in our measurements. We find (as discussed below) that the magnetic field in the subarcsecond and arcsecond scale jets is always initially parallel to the jet axis. If the misalignments between VLBI and arcsecond/subarcsecond scales are, in general, not very large, this could explain the observed correlation found by Rusk and Seaquist (1985) and Jones et al. (1985). However, in general, the misalignments between the VLBI and arcsecond-scale structure of coredominated sources are fairly large (Fig. 21 below; also Jones et al.; Rusk and Rusk 1986). Thus, confusion probably contributes only a small amount to the discrepancy.

A third possibility for the wavelength dependence of the alignment is that the polarized structure whose B field is aligned with the milliarcsecond VLBI jet (possibly the VLBI jet itself) has a steep spectral index. The lack of an alignment at 1.3 cm may reflect the lack of polarized extended structure at that short wavelength. This should be tested with VLBI polarization observations.

# b) The Magnetic Field in the Arcsecond-Scale Jets

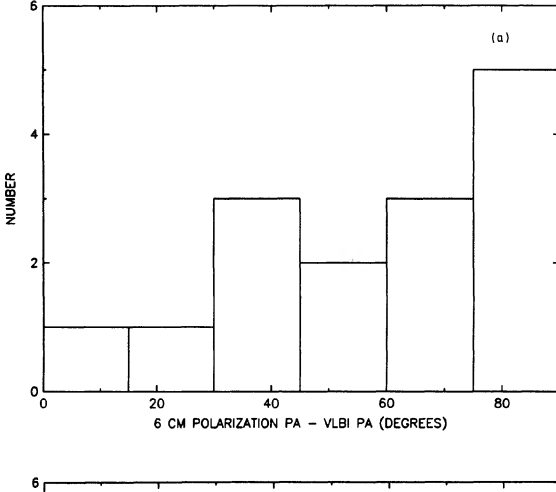
In all of the jets with data of sufficient quality, we see that the magnetic field is initially parallel to the jet axis. If this field configuration is maintained between the milliarcsecond and arcsecond size scales, this places the strongest constraints on the evolution (with beam radius  $r_b$  and velocity  $v_b$ ) of the B field, since the parallel component of the B field evolves as  $B_{\parallel} \propto r_b^{-2}$  while the perpendicular component evolves as  $B_{\perp} \propto v_b^{-1} r_b^{-1}$  (e.g., Blandford and Rees 1974). Thus, between the parsec and kiloparsec scales,  $B_{\parallel}$  should decline by a factor of  $\sim 10^6$ , while  $B_{\perp}$  will decline by a factor of  $\sim 10^3$  in a constant-velocity jet.

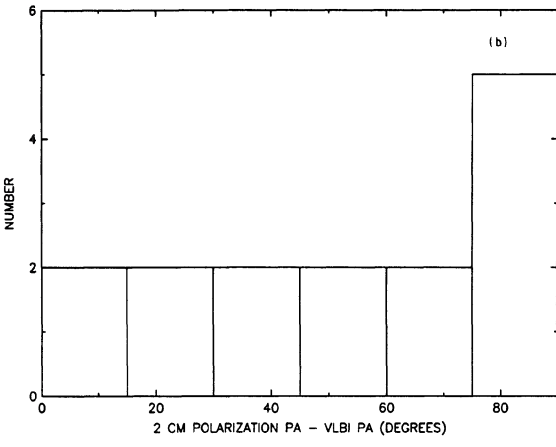
We estimate magnetic fields corresponding to minimum pressure in the arcsecond jets and lobes of  $\sim 50~\mu G$  (Table III). This can be compared with the estimated field strengths in milliarcsecond jets of  $\sim 5\times 10^4~\mu G$  (e.g., Linfield 1982; Unwin et al. 1985). The ratio is a factor of  $\sim 10^3$  rather than a factor of  $\sim 10^6$ . This is more consistent with the variation expected from the  $B_1$  configuration rather than the observed  $B_{\parallel}$  configuration. One possible explanation is that the magnetic field is generated in the jet. A second possibility is that some process (e.g., turbulence or shearing of the B field by velocity gradients across the jet) can transfer energy from the perpendicular to parallel components and preserve the appearance of a  $B_{\parallel}$  configuration while reducing the expansion losses of magnetic flux density (e.g., as suggested for the jets in NGC 1265 by O'Dea and Owen 1987).

## c) Precession or Instabilities?

The wiggles in 1823 + 568 and 2037 + 511 are of large projected amplitude and may be caused by precession of the

450





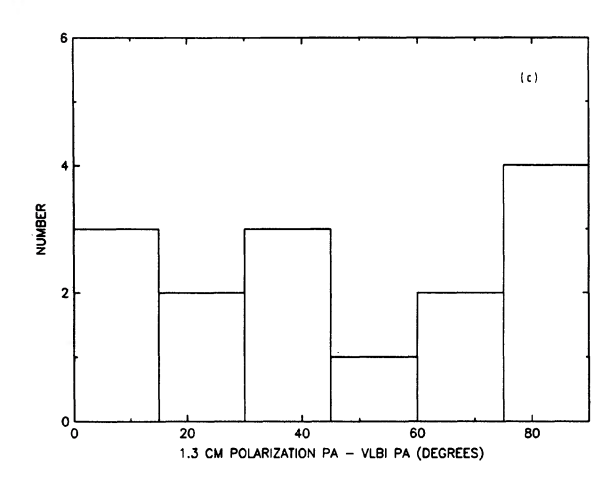


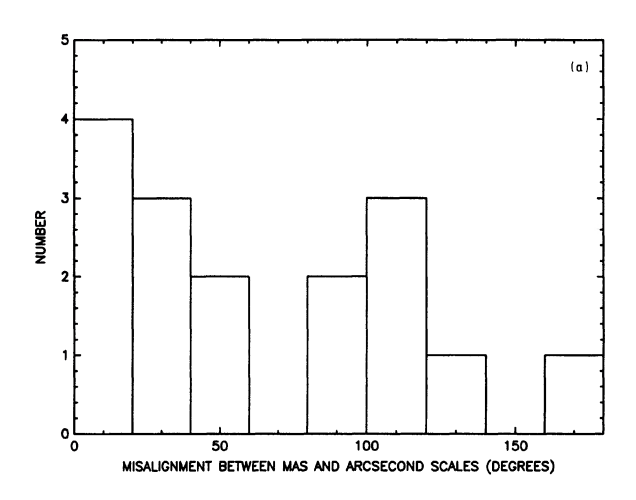
FIG. 20. (a) A histogram of the difference between the 6 cm polarization position angle of the core and the orientation of the VLBI structure (from Table II). (b) Same for 2 cm. (c) Same for 1.3 cm.

central engine with the ejected material following a ballistic trajectory. Muxlow et al. (1984) have fit such a model to the wiggle in 2037 + 511. However, it is also possible that the wiggles are caused by Kelvin-Helmholtz instabilities in a continuous jet (e.g., Benford 1981; Ferrari, Trusoni, and Zanninetti 1983; Hardee 1986, 1987; Ray 1981). Can the

magnetic field structure be used to decide between these two possibilities?

In the case of ballistic motion and a precessing engine, the expected magnetic field structure is not obvious. However, the magnetic field structure may be determined by the interaction of the local piece of plasma with the ambient medium. Since the plasma will be compressed in the direction of its motion, we might expect the magnetic field to be locally perpendicular to the direction to the core.

In the case of a continuous fluid beam, if the magnetic field is unimportant dynamically, the magnetic field structure will be determined by the velocity field of the beam. Generally, in jets that interact strongly with an ambient medium along their edges, the magnetic field will be stretched or sheared in the direction of the fluid motion, i.e., along the axis of the jet. This behavior is seen in bent jets in, for example, the tailed radio galaxies NGC 1265 (O'Dea and Owen 1986) and 1919 + 479 (Burns et al. 1986) and the quasar



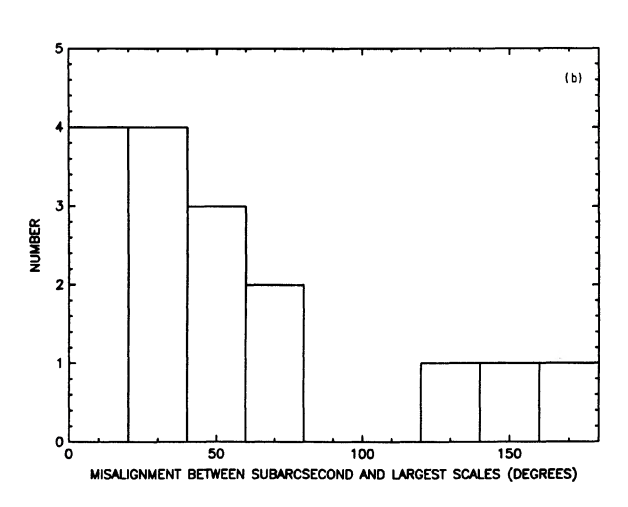


FIG. 21. (a) A histogram of the difference between the orientation of the milliarcsecond (Table II) and arcsecond structure (Table III). (b) A histogram of the difference between the orientation of the structure found closest to and furthest from the core on the subarcsecond to largest scales (Table III).

1857 + 566 (Saikia *et al.* 1983), as well as in the outer edges of bent jets in 3C 31 (Burch 1979; Strom *et al.* 1983) and NGC 6251 (Perley, Bridle, and Willis 1984).

In 1823 + 568 and 2037 + 511, the magnetic field is generally parallel to the jet axis and follows the local curvature of the jets. The magnetic field takes on a different orientation at or near the knots; however, the knots may represent (possibly oblique) shocks in the jets which will locally compress the jet fluid and change the orientation of the projected magnetic field. (Projection effects as the jet twists in three dimensions may also cause some departure from an apparently axial field.) Thus, the magnetic field structures in 1823 + 568 and 2037 + 511 are consistent with fluid instabilities in a continuous beam. However, we cannot rule out precession of the central engine as the cause of the wiggles.

## d) Misalignments and Bending

A histogram of the position-angle differences between the milliarcseond (Table II) and arcsecond (Table III) structure for our 16 sources is given in Fig. 21(a). The distribution of observed position-angle differences is fairly flat. In six of the 16 sources, the milliarcsecond structure is misaligned by  $\geq 90^{\circ}$  with the arcsecond structure. These large position-angle differences need not be *intrinsic* since projection effects can enhance the apparent misalignments (Readhead *et al.* 1978; Moore *et al.* 1981; Browne *et al.* 1982a; Readhead *et al.* 1983; Rusk and Rusk 1986).

The distribution of misalignments between milliarcsecond and arcsecond structure can potentially constrain the source geometry (e.g., Moore et al. 1981). However, in practice, this is difficult since the inferred values of the inclination angle and intrinsic bending angle are coupled (Rusk and Rusk 1986). The large misalignments indicated in Fig. 21(a) are consistent with the hypothesis that, in general, the jets are oriented at a small angle to the line of sight, though the hypothesis that the sources have large intrinsic bends cannot currently be ruled out.

Our VLA observations (Figs. 1–19) indicate that substantial curvature is found on the arcsecond scales as well as on the milliarcsecond scales (see also, e.g., Walker, Benson, and Unwin 1987; Browne et al. 1982a; Foley 1982). Table III and Fig. 21(b) give the misalignments between the structure closest to and furthest from the core seen in the VLA images. Figure 21 suggests that the amount of bending on the large and small scales is similar, though possibly somewhat less on the larger scales. However, a two-sided, two-sample Kolmogorov–Smirnov test gives a probability of 23% that the null hypothesis (i.e., that the two distributions are the same) is correct.

If the selection for core dominance results in a preference for sources whose milliarcsecond jets are oriented fairly closely to our line of sight, then, statistically, any bending of the larger-scale structure would be more likely to increase rather than decrease its inclination to our line of sight. This would cause a decrease in the amount of apparent bending on larger scales. However, there is only a hint from the present data that the large-scale structure is oriented at a larger angle to the line of sight than the milliarcsecond structure (as suggested by Schilizzi and de Bruyn 1983). If confirmed, this would suggest that the angular sizes of the extended structure should not be deprojected using the inclination derived for the milliarcsecond structure.

e) What is the Connection with Lobe-Dominated Sources?

1) Properties of the extended emission

From a study of 125 mainly lobe-dominated sources, Bridle (1984) found that radio sources with core powers\* at 5 GHz above  $10^{23.3}$  W Hz<sup>-1</sup>, or, equivalently, total powers at 1.4 GHz above  $10^{24.8}$  W Hz<sup>-1</sup>, have apparently one-sided rather than two-sided jets and tend to have magnetic field structures that are parallel to the jet axis for essentially the entire length of the jet. Sources at these high powers are also expected to exhibit Fanaroff and Riley (1974) class II (i.e., classical double) morphologies.

Although our sources are core dominated, the powers of the *extended* emission (Table III) are themselves very large (median power  $\sim 10^{26.7}$  W Hz<sup>-1</sup> at 1.4 GHz). This is not too surprising since ten of the 16 sources are found in the 4C or 3C catalogs. These sources should be powerful classical doubles based on the flux density of their extended structure. Unless the flux density of the extended structure is Doppler boosted by a factor of more than  $\sim 100$ , the parent population of the core-dominated quasars must include classical double quasars, if the unifying scheme is correct.

The issue of whether or not the core-dominated quasars exhibit extended structure that is compatible with classical double source structure has been discussed by PFJ80 and PFJ82. Our results are consistent with their findings that the extended structure of core-dominated sources is observed to be more asymmetric than (or perhaps simply different from) the extended structure of lobe-dominated sources. As we note in Sec. IV, two-sided "classical double" structure is seen in 0224 + 671,0859 - 140,1055 + 018,1633 + 382, and 1642 + 690. However, the nine other powerful sources do not show structure that is obviously classical double. PFJ80 and PFJ82 examine two hypotheses. The first hypothesis is that the core-dominated sources are an intrinsically different population of objects from the lobe-dominated sources. The second hypothesis is that the unifying scheme is correct and the core-dominated sources are drawn from a parent population of lobe-dominated sources in which beaming effects are important in both the core and the extended structure. Our results do not discriminate between these two hypotheses; however, as we point out below, if the unifying scheme is correct, at least moderately relativistic velocities must persist out to scales of tens of kpc in these sources

In addition, if Bridle's (1984) relationships extrapolate to core-dominated sources, the sources are expected to have apparently one-sided jets and projected magnetic fields that are parallel to the jet axis for the entire length of the jet. Our observations are basically consistent with these expectations. However, we note that in 0605-085, 1642+690, and 1823+568, the magnetic field does not remain parallel to the jet axis for the full length of the jet, contrary to the trend for sources of such high radio power (Bridle 1984). This might be an effect of our limited spatial resolution if the end of the jet is embedded in a lobe or cocoon that has a perpendicular magnetic field and our resolution blends the polarization from both the jet and lobe.

2) Constraints on velocity from one-sidedness

On the angular scales sampled by these observations, the sources do have one-sided jets or secondary components.

<sup>\*</sup>Powers corrected for  $H_0 = 75 \text{ km s}^{-1} \text{ Mpc}^{-1}$ .

<sup>†</sup> High-resolution observations may have resolved out diffuse structure which, if seen, would give these sources a classical double appearance.

452

One-sided jets are found in 0224+671, 0605-085, 0735+178, 1055+018, 1510-089, 1633+382, 1642+690, 1807+698, 1823+568, and 2037+511. Short extensions to the core which may be jets are found in 1624+416 and 1749+701; and 0333+321, 0836+710, 0859-140, and 1116+128 have single secondary components that are much brighter than any possible countercomponent. The observed peak ratio between the surface brightness of the two sides of the source (Sec. IIIb) is given in Table III.

If these 16 sources are intrinsically symmetric, then the relative Doppler boosting of the surface brightness of the two jets  $R_{1/2}$  is given by (Blandford and Königl 1979)

$$R_{1/2} = \left(\frac{1 + \beta \cos(\theta)}{1 - \beta \cos(\theta)}\right)^{2 - \alpha}.$$
 (1)

The constraint on the bulk velocity is given by

$$\beta \cos \theta = \frac{R_{1/2}^{\gamma} - 1}{1 + R_{1/2}^{\gamma}},\tag{2}$$

where  $\gamma = (2 - \alpha)^{-1}$  and we adopt  $\alpha = -0.75$  for the spectral index of the extended structure. The resulting constraint on the bulk velocity is given in Table III for these sources. If the sources are intrinsically asymmetric, then the velocity may be overestimated (depending on the sense of the asymmetry). However, for many sources we have only lower limits to the side-to-side brightness ratios since only one jet or lobe is detected. The median lower limit to the sideto-side brightness asymmetry is  $\sim 10$ , though the values range up to  $\sim 100$  (Table III). The observed limits on asymmetry correspond to lower limits to  $\beta$  of 0.2–0.7 for  $\theta = 0.0$ . Larger values of  $\beta$  are required for larger inclinations to the line to sight. Thus, the Doppler boosting of the extended structure (or at least the jets) may be larger than previously thought. Browne and Perley (1986) estimate  $\beta \sim 0.2$  for the extended structure in their sample of 135 core-dominated sources. Part of this difference may be that we have detected one-sided jets, while the structures used by Browne and Perley in their estimate were mainly diffuse or secondary components with smaller asymmetries.

Bulk velocities larger than  $\beta \sim 0.3$  in the *extended* structure have been argued against by Moore *et al.* (1981) and Browne and Perley (1986) based on constraints on the advance speeds of hotspots in classical double sources. They note that statistical arguments based on lobe-core separation ratios (Longair and Riley 1979; Banhatti 1980; Gopal-Krishna 1980; Macklin 1981) suggest lobe-advance speeds of no more than  $\beta \sim 0.3$ . In addition, ram-pressure balance between the lobes and external medium also favors low advance speeds (e.g., Browne and Perley 1986).

However, other re-examinations of the distribution of lobe-core separation ratios suggest that this statistic may not be useful for constraining lobe-advance speeds (Baryshev 1983; Fokker 1986). Moreover, we wish to point out that it is the *flow* speeds and not the *advance* speeds that are physically important in determining Doppler boosting of the surface brightnesses. In any realistic beam model, the flow speed in the jet is much larger than the advance speed of the hotspot (e.g., Begelman, Blandford, and Rees 1984). Numerical hydrodynamic models of hotspots (Smith *et al.* 1985) indicate that the shock pattern (and resulting flow pattern) in hotspots can be very complex. The flow speed of the material in the hotspot can remain very large (a significant fraction of the initial jet speed), especially if the hotspot contains oblique shocks (e.g., Smith *et al.* 1985; Lind 1986, and pri-

vate communication). Thus, the surface-brightness ratios between opposing sides will be enhanced by the fastest-moving material in the jets, hotspots, and lobes, and can be much larger than otherwise expected. The effects of Doppler boosting in the extended structure should be incorporated into the unifying schemes.

## VI. SUMMARY AND CONCLUDING REMARKS

We present subarcsecond-resolution VLA observations at wavelengths of 6, 2, and 1.3 cm of 16 core-dominated quasars and active galactic nuclei. We have detected a wide variety of structures, including one-sided jets, short extensions to the cores, which may be jets, and secondary components, which may be hotspots or the brighter parts of lobes.

The magnetic fields in the jets are always initially parallel to the jet axis at the base of the jets and continue to be parallel for most sources even as the jets bend. We suggest that this magnetic field structure is consistent with an explanation for the wiggles of the jets in 1823 + 568 and 2037 + 511 in terms of helical instabilities in a fluid beam. However, we cannot rule out precession of the central engine with ballistic motion of the ejecta as the cause of the apparent wiggles.

We find no tendency for the 1.3 cm polarization position angle of the *core* to be perpendicular to the milliarcsecond radio-source axis. This is in contrast with previous results based on lower-frequency observations. The discrepancy may be caused by increased variability or by a lack of extended polarized structure whose *B* field is aligned with the VLBI jet at short wavelengths.

We find significant curvature in the structure on subarcsecond and arcsecond scales. The amount of misalignment seen on these scales is similar to (but perhaps slightly smaller than) that inferred on the milliarcsecond to subarcsecond scales.

The powers of the extended emission of these objects are sufficiently large that the sources should exhibit one-sided jets with magnetic fields aligned with the axis of the jet (Bridle 1984). For most of our sources, our results are consistent with these properties.

Based on the large powers of the extended emission, these sources should also have Fanaroff and Riley class II (classical double) morphology. However, consistent with previous work (e.g., PFJ80, PFJ82), we find that the extended structure of these core-dominated sources is more asymmetric than the extended structure of lobe-dominated sources. The asymmetry between opposing sides of the sources suggests that the jets and secondary components (if they are intrinsically symmetric) contain material that has bulk velocities  $\beta$  $\cos \theta \sim 0.2$ –0.7. We note that previous limits on the expected Doppler boosting in the extended structure based on advance speeds of the hotspots may be in error. We point out that numerical hydrodynamic models of hotspots as well as analytic arguments suggest that the flow speeds through the hotspots will be a substantial fraction of the initial jet velocity. Thus, Doppler boosting of the extended structure can be important and should be incorporated in the unifying schemes.

We thank Tom Balonek for his interest during the early stages of the project, and Stefi Baum, Joan Wrobel, and Colin Lonsdale for comments on the manuscript. Critical comments by Larry Rudnick helped to focus our discussion. We are grateful to Dave Murphy, Joan Wrobel, and Susan Neff for sharing their results in advance of publication, and to Kevin Lind for useful suggestions.

453

#### REFERENCES

- Aller, H. D., Aller, M. F., Latimer, G. E., and Hodge, P. E. (1985). Astrophys. J. Suppl. 59, 513.
- Antonucci, R. R. J., and Ulvestad, J. S. (1985). Astrophys. J. 294, 158. Baars, J. W. M., Genzel, R., Pauliny-Toth, I. I. K., and Witzel, A. (1977). Astron. Astrophys. 61, 99.
- Bååth, L. B. (1984). In VLBI and Compact Radio Sources, IAU Symposium No. 110, edited by R. Fanti, K. Kellerman, and G. Setti (Reidel, Dordrecht), p. 127.
- Banhatti, D. G. (1980). Astron. Astrophys. 84, 112.
- Baryshev, Yu. V. (1983). Astrofizika 19, 461. (English translation (1984). Astrophysics 19, 257).
- Begelman, M. C., Blandford, R. D., and Rees, M. J. (1984). Rev. Mod. Phys. 56, 255.
- Benford, G. (1981). Astrophys. J. 247, 792.
- Blandford, R. D., and Königl, A. (1979). Astrophys. J. 232, 34.
- Blandford, R. D., and Rees, M. J. (1974). Mon. Not. R. Astron. Soc. 169, 395.
- Blandford, R. D., and Rees, M. J. (1978). In *Pittsburgh Conference on BL Lac Objects*, edited by A. M. Wolfe (University of Pittsburgh, Pittsburgh), p. 328.
- Bridle, A. H. (1984). Astron. J. 89, 979.
- Bridle, A. H., and Eilek, J. A., editors (1985). In Physics of Energy Transport in Extragalactic Radio Sources, Proceedings of NRAO Workshop No. 9 (NRAO, Green Bank, WV).
- Bridle, A. H., and Perley, R. A. (1984). Annu. Rev. Astron. Astrophys. 22, 319.
- Browne, I. W. A., (1987). In Superluminal Radio Sources, edited by J. A. Zensus and T. J. Pearson (Cambridge University, Cambridge), p. 129.
- Browne, I. W. A., and Orr, M. J. L. (1981). In *Optical Jets in Galaxies*, ESA SP-162 (European Space Agency, Paris), p. 87.
- Browne, I. W. A., Clark, R. R., Moore, P. K., Muxlow, T. W. B., Wilkinson, P. N., Cohen, M. H., and Porcas, R. W. (1982b). Nature 299, 788.
- Browne, I. W. A., Orr, M. J. L., Davis, R. J., Foley, A., Muxlow, T. W. B., and Thomasson, P. (1982a). Mon. Not. R. Astron. Soc. 198, 673.
- Browne, I. W. A., and Perley, R. A. (1986). Mon. Not. R. Astron. Soc. 222,
- Burch, S. F. (1979). Mon. Not. R. Astron. Soc. 187, 187.
- Burns, J. O., O'Dea, C. P., Gregory, S. A., and Balonek, T. J. (1986). Astrophys. J. 307, 73.
- Burns, J. O., Owen, F. N., and Rudnick, L. (1979). Astron. J. 84, 1683. Clark, B. G. (1980). Astron. Astrophys. 89, 399.
- Dreher, J. W. (1981). Astron. J. 86, 833.
- Eckart, A., Witzel, A., Biermann, P., Johnston, K. J., Simon, R., Schalinski, C., and Kuhr, H. (1987). Astron. Astrophys. Suppl. 67, 121.
- Fanaroff, B. L., and Riley, J. M. (1974). Mon. Not. R. Astron. Soc. 167, 31P
- Ferrari, A., Trussoni, E., and Zaninetti, L. (1983). Astron. Astrophys. 125, 179
- Foley, A. R. (1982). Ph. D. dissertation, University of Manchester.
- Fokker, A. D. (1986). Astron. Astrophys. 156, 315.
- Gopal-Krishna (1980). Astron. Astrophys. 86, L1.
- Hardee, P. E. (1986). Can. J. Phys. 64, 484.
- Hardee, P. E. (1987). Astrophys. J. 318, 78.
- Hewitt, A., and Burbidge, G. (1987). Astrophys. J. Suppl. 63, 1.
- Jones, T. W., Rudnick, L., Aller, H. D., Aller, M. F., Hodge, P. E., and Fiedler, R. L. (1985). Astrophys. J. 290, 627.
- Kellermann, K. I., Shaffer, D. B., Purcell, G. H., Pauliny-Toth, I. I. K., Preuss, E., Witzel, A., Graham, D., Schilizzi, R. T., Cohen, M. H., Moffet, A. T., Romney, J. D., and Neil, A. E. (1977). Astrophys. J. 211, 658.
- Killeen, N. E. B., Bicknell, G. V., and Ekers, R. D. (1986). Astrophys. J. 302, 306.
- Lebofsky, M. J., Rieke, G. H., and Walsh, D. (1983). Mon. Not. R. Astron. Soc. 203, 727.
- Lind, K. (1986). Ph. D. dissertation, California Institute of Technology.
- Lind, K. (1987). In Superluminal Radio Sources, edited by J. A. Zensus and T. J. Pearson (Cambridge University, Cambridge), p. 180.
- Linfield, R. (1982). Astrophys. J. 254, 465.
- Longair, M. S., and Riley, J. M. (1979). Mon. Not. R. Astron. Soc. 188, 625.

- Macklin, J. T. (1981). Mon. Not. R. Astron. Soc. 196, 967.
- Marscher, A. P., and Broderick, J. J. (1985). Astrophys. J. 290, 735.
- Moore, P. K., Browne, I. W. A., Daintree, E. J., Noble, R. G., and Walsh, D. (1981). Mon. Not. R. Astron. Soc. 197, 325.
- Murphy, D. W. (1988). Ph. D. dissertation, University of Manchester.
- Muxlow, T. W. B., Jullian, M., and Linfield, R. (1984). In VLBI and Compact Radio Sources, IAU Symposium No. 110, edited by R. Fanti, K. Kellerman, and G. Setti (Reidel, Dordrecht), p. 141.
- O'Dea, C. P., and Owen, F. N. (1986). Astrophys. J. 301, 841.
- O'Dea, C. P., and Owen, F. N. (1987). Astrophys. J. 316, 95.
- Orr, M. J. L., and Browne, I. W. A. (1982). Mon. Not. R. Astron. Soc. 200, 1067.
- Padrielli, L., Romney, J. D., Bartel, N., Fanti, R., Ficarra, A., Mantovani, F., Matveyenko, L., Nicholson, G. D., and Weiler, K. W. (1986). Astron. Astrophys. 165, 53.
- Peacock, J. A., Perryman, M. A. C., Longair, M. S., Gunn, J. E., and Westphal, J. A. (1981). Mon. Not. R. Astron. Soc. 194, 601.
- Pearson, T. J., Barthel, P. D., Lawrence, C. R., and Readhead, A. C. S. (1986). Astrophys. J. Lett. 300, L25.
- Pearson, T. J., Perley, R. A., and Readhead, A. C. S. (1985). Astron. J. 90, 738.
- Pearson, T. J., and Readhead, A. C. S. (1981). Astrophys. J. 248, 61.
- Perley, R. A. (1982). Astron. J. 87, 859.
- Perley, R. A., Bridle, A. H., and Willis, A. G. (1984). Astrophys. J. Suppl. 54, 291.
- Perley, R. A., Fomalont, E. B., and Johnston, K. J. (1980). Astron. J. 85, 649 (PFJ80).
- Perley, R. A., Fomalont, E. B., and Johnston, K. J. 1982 Astrophys. J. Lett. 255, 193.
- Pilbratt, G., Booth, R. S., and Porcas, R. W. (1987). Astron. Astrophys. 173, 12.
- Ray, T. P. (1981). Mon. Not. R. Astron. Soc. 196, 195.
- Readhead, A. C. S., Cohen, M. H., Pearson, T. J., and Wilkinson, P. N. (1978). Nature 276, 768.
- Readhead, A. C. S., Hough, D. H., Ewing, M. S., Walker, R. C., and Romney, J. D. (1983). Astrophys. J. 265, 107.
- Romney, J., Padrielli, L., Bartel, N., Weiler, K. W., Ficarra, A., Mantovani, F., Bååth, L. B., Kogan, L., Matveyenko, L., Moiseev, I. G., and Nicholson, G. (1984). Astron. Astrophys. 135, 289.
- Rudnick, L., and Jones, T. W. (1983). Astron. J. 88, 518.
- Rudnick, L., Jones, T. W., Aller, H. D., Aller, M. F., Hodge, P. E., Owen, F. N., Fiedler, R. L., Puschell, J. J., and Bignell, R. C. (1985). Astrophys. J. Suppl. 57, 693.
- Rusk, R., and Rusk, A. C. M. (1986). Can. J. Phys. 64, 440.
- Rusk, R., and Seaquist, E. R. (1985). Astron. J. 90, 30.
- Saikia, D. J., Shastri, P., Cornwell, T. J., and Banhatti, D. G. (1983). Mon. Not. R. Astron. Soc. 203, 53P.
- Scheuer, P. A. G. (1987). In Superluminal Radio Sources, edited by J. A. Zensus and T. J. Pearson (Cambridge University, Cambridge), p. 104.
- Schilizzi, R. T., and de Bruyn, A. G. (1983). Nature 303, 26.
- Schwab, F. (1980). Proc. SPIE 231, 18.
- Simard-Normandin, M., Kronberg, P. P., and Button, S. (1981). Astrophys. J. Suppl. 45, 97.
- Smith, M. D., Norman, M. L., Winkler, K-H. A., and Smarr, L. (1985).
  Mon. Not. R. Astron. Soc. 214, 67.
- Strom, R. G., Fanti, R., Parma, P., and Ekers, R. D. (1983). Astron. Astrophys. 122, 305.
- Thompson, A. R., Clark, B. G., Wade, C. M., and Napier, P. J. (1980). Astrophys. J. Suppl. 44, 151.
- Ulvestad, J. S., and Johnston, K. J. (1984). Astron. J. 89, 189.
- Unwin, S. C., Cohen, M. H., Biretta, J. A., Pearson, T. J., Seielstad, G. A., Walker, R. C., Simon, R. S., and Linfield, R. P. (1985). Astrophys. J. 280, 109
- Véron-Cetty, M.-P., and Véron, P. (1987). ESO Sci. Rep. No. 5.
- Walker, R. C., Benson, J. M., and Unwin, S. C. (1987). Astrophys. J. 316, 546.
- Wilkinson, P. N. (1982). In Extragalactic Radio Sources, IAU Symposium No. 97, edited by D. Heeschen and C. M. Wade (Reidel, Dordrecht), p. 140

Witzel, A. (1987). In Superluminal Radio Sources, edited by J. A. Zensus and T. J. Pearson (Cambridge University, Cambridge), p. 83.
Wrobel, J. M. (1987). In Superluminal Radio Sources, edited by J. A. Zensus and T. J. Pearson (Cambridge University, Cambridge), p. 186.
Wrobel, J. M., Pearson, T. J., Cohen, M. H., and Readhead, A. C. S.

(1988). In *The Impact of VLBI on Astrophysics and Geophysics*, IAU Symposium No. 129, edited by M. Reid and J. Moran (Reidel, Dordrecht) (in press).

Zensus, J. A., Porcas, R. W., and Pauliny-Toth, I. I. K. (1984). Astron. Astrophys. 133, 27.